A Novel Expression Domain of *extradenticle* Underlies the Evolutionary Developmental Origin of the Chelicerate Patella

Benjamin C. Klementz [1,2,*] Georg Brenneis [3] Isaac A. Hinne [4] Ethan M. Laumer,[1,2] Sophie M. Neu,[1,2] Grace M. Hareid [1,2] Guilherme Gainett [1,5,6] Emily V.W. Setton [1,7] Catalina Simian [8] David E. Vrech [8] Isabella Joyce,[9] Austen A. Barnett [9] Nipam H. Patel [10,11] Mark S. Harvey [12] Alfredo V. Peretti [8] Monika Gulia-Nuss [4] Prashant P. Sharma [1,2]

[1]Department of Integrative Biology, University of Wisconsin-Madison, Madison, WI, USA
[2]University of Wisconsin-Madison Zoological Museum, University of Wisconsin-Madison, Madison, WI, USA
[3]Unit Integrative Zoologie, Department Evolutionsbiologie, Universität Wien, Vienna, Austria
[4]Department of Biochemistry and Molecular Biology, University of Nevada, Reno, NV, USA
[5]Department of Systems Biology, Harvard Medical School, Boston, MA, USA
[6]Department of Pathology, Boston Children,'s Hospital, Boston, MA, USA
[7]Department of Ecology and Evolutionary Biology, Cornell University, Ithaca, NY, USA
[8]Laboratorio de Biología Reproductiva y Evolución, Instituto de Diversidad y Ecología Animal (IDEA), Consejo Nacional de Investigaciones Científicas Técnicas (CONICET), Universidad Nacional de Córdoba, Córdoba, Argentina
[9]Department of Biology, DeSales University, Center Valley, PA, USA
[10]Marine Biological Laboratory, Woods Hole, MA, USA
[11]Organismal Biology & Anatomy, University of Chicago, Chicago, IL, USA
[12]Collections & Research, Western Australian Museum, Welshpool, WA, Australia

***Corresponding author:** E-mail: bklementz@wisc.edu.

Associate editor: John True

Abstract

Neofunctionalization of duplicated gene copies is thought to be an important process underlying the origin of evolutionary novelty and provides an elegant mechanism for the origin of new phenotypic traits. One putative case where a new gene copy has been linked to a novel morphological trait is the origin of the arachnid patella, a taxonomically restricted leg segment. In spiders, the origin of this segment has been linked to the origin of the paralog *dachshund-2*, suggesting that a new gene facilitated the expression of a new trait. However, various arachnid groups that possess patellae do not have a copy of *dachshund-2*, disfavoring the direct link between gene origin and trait origin. We investigated the developmental genetic basis for patellar patterning in the harvestman *Phalangium opilio*, which lacks *dachshund-2*. Here, we show that the harvestman patella is established by a novel expression domain of the transcription factor *extradenticle*. Leveraging this definition of patellar identity, we surveyed targeted groups across chelicerate phylogeny to assess when this trait evolved. We show that a patellar homolog is present in Pycnogonida (sea spiders) and various arachnid orders, suggesting a single origin of the patella in the ancestor of Chelicerata. A potential loss of the patella is observed in Ixodida. Our results suggest that the modification of an ancient gene, rather than the neofunctionalization of a new gene copy, underlies the origin of the patella. Broadly, this work underscores the value of comparative data and broad taxonomic sampling when testing hypotheses in evolutionary developmental biology.

Downloaded from https://academic.oup.com/mbe/article/41/9/msae188/7750... by guest on 04 October 2024

Received: May 16, 2024. **Revised:** August 02, 2024. **Accepted:** August 30, 2024
© The Author(s) 2024. Published by Oxford University Press on behalf of Society for Molecular Biology and Evolution.
This is an Open Access article distributed under the terms of the Creative Commons Attribution License (https://creativecommons.org/licenses/by/4.0/), which permits unrestricted reuse, distribution, and reproduction in any medium, provided the original work is properly cited.

Discoveries

Open Access

Graphical abstract

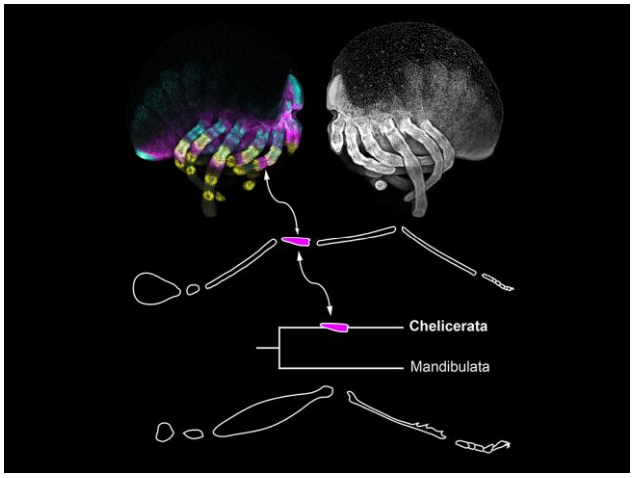

***Key words: dachshund*, daddy longlegs, Pycnogonida, segmentation, subfunctionalization.**

Introduction

One of the central goals of evolutionary developmental biology remains demonstrating the mechanistic basis by which evolutionary novelty arises, including both morphological and molecular innovation through modifications of development (reviewed in Hall [2012]). Two competing hypotheses pertain to the genetic basis for the origin of novelty. The first is the acquisition of a novel function by an existing gene. This can be accomplished via diverse mechanisms, including heterochrony (de Beer 1930; Raff 1992; MacDonald and Hall 2001; Smith 2003; Tills et al. 2011), the modification of gene expression domains (Carpio et al. 2004; Janssen et al. 2021), alterations in *cis* regulatory interactions (Mazo-Vargas et al. 2022; Tendolkar et al. 2024), and the co-option of existing gene regulatory networks (Moczek and Rose 2009; Setton and Sharma 2018). The second explanation ties evolutionary novelty with the birth of new genes, with new functions either generated de novo (Cai et al. 2008; Knowles and McLysaght 2009) or via divergence following tandem or whole genome duplication events (Haldane 1990; Dittmar and Liberles 2011). While pseudogenization and eventual loss are understood to be the most likely long-term outcome for duplicated genes (Ohno 1970; Brunet et al. 2006; Gout et al. 2023), copies that persist may either subdivide the ancestral gene's function (subfunctionalization) and thereby reduce pleiotropy, or one daughter copy may acquire a novel function (neofunctionalization) (Lynch and Conery 2000). These processes are non-mutually exclusive and may act in tandem (He and Zhang 2005). However, neofunctionalization of new gene copies is an especially compelling phenomenon when it is linked to novel traits.

One prominent case of neofunctionalization appears to underly the origin of the patella, a segment (or podomere) found in the pedipalps and walking legs of a subset of chelicerate arthropods (sea spiders, horseshoe crabs, and terrestrial arachnids) (Turetzek et al. 2016) (fig. 1*a*). Much of the evolutionary success of Arthropoda, the most species-rich of the metazoan phyla, can be attributed to their eponymous jointed appendages. Subdivision of these appendages into discrete, sclerotized podomeres not only improves appendage flexibility and range of motion but also provides additional substrates for morphological innovation and regionalization (Brusca and Brusca 2003). This regionalization has given rise to a wide range of appendage forms and functions, including modification of the first pair of walking legs into the venom-injecting forcipules of centipedes, the raptorial appendages of mantis shrimps, the grasping pedipalps of scorpions, or the antenniform sensory legs of whip spiders and vinegaroons, ultimately enabling the phylum to exploit all but the most extreme habitats. The presence of the patella, however, differentiates the six-segmented leg of a typical mandibulate arthropod (myriapods, crustaceans, and insects) from the seven-segmented walking legs of arachnids like spiders and scorpions. Chelicerate pedipalps also possess a patella but are six-segmented due to absence of the metatarsal segment.

The evolutionary origin of the patella was recently inferred to result from the neofunctionalization of a duplicated paralog of the conserved appendage patterning gene *dachshund* (*dac*) (Turetzek et al. 2016). During establishment of the arthropod proximo-distal (PD) limb axis, *dac* is one of four primary transcription factors (alongside *homothorax* (*hth*), *extradenticle* (*exd*), and *Distal-less* (*Dll*)), that regionalizes the PD axis; in the fruit fly *Drosophila melanogaster*, the canonical *dac* loss-of-function phenotype exhibits a deletion of medial segments (Dong et al. 2001). Bioinformatic and gene expression surveys have also inferred that a single copy of *dac* was present in the common ancestor of Panarthropoda (Tardigrada, Onychophora, and Arthropoda) (Prpic and Tautz 2003; Angelini and Kaufman 2005; Janssen et al. 2010; Sharma

Downloaded from https://academic.oup.com/mbe/article/41/9/msae188/7749772 by guest on 11 October 2024

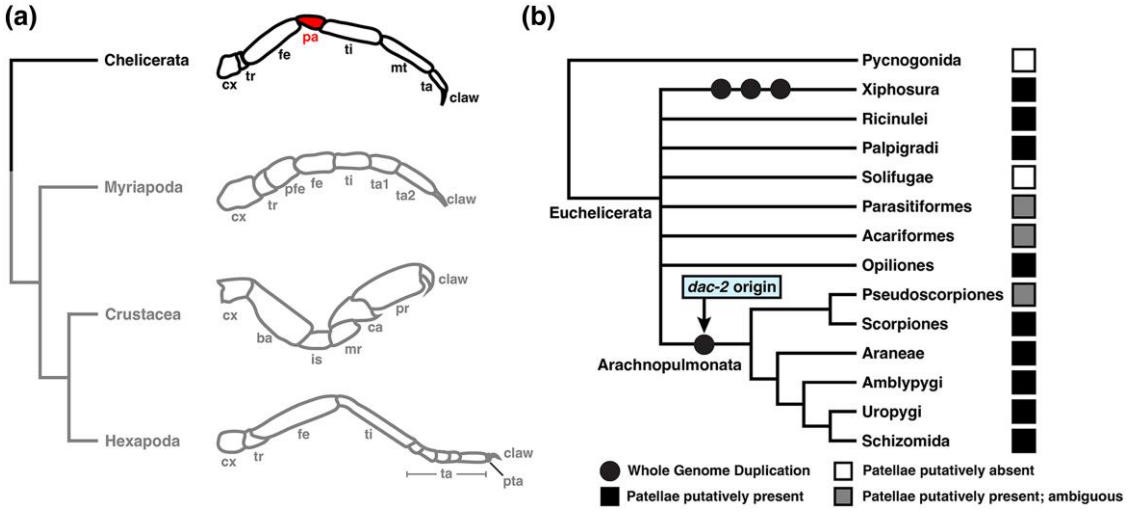

Fig. 1. The patella differentiates the appendages of most chelicerate orders from other arthropods. (**a**) Exemplars of leg architecture across major arthropod lineages. Appendage schematics from top to bottom: spider leg; centipede leg; amphipod cheliped; insect leg. (**b**) Simplified phylogeny of Chelicerata. Icons indicate condition of patella. Origin of *dac-2* has been inferred to originate from whole-genome duplication in the arachnopulmonate ancestor. Abbreviations: cx, coxa; tr, trochanter; fe, femur; pa, patella; ti, tibia; mt, metatarsus; ta, tarsus; pfe, prefemur; ba, basis; is, ischium; mr, merus; ca, carpus; pr, propodus; pta, pretarsus. Chelicerate tree topology based on Ballesteros et al. (2022) with unstable nodes collapsed.

et al. 2012a; Barnett and Thomas 2013). Previous functional studies in pancrustaceans and one arachnid species demonstrated a conserved role for *dac* in patterning the medial territory of the walking leg across Arthropoda (Angelini and Kaufman 2004; Sewell et al. 2008; Angelini et al. 2009, 2012; Sharma et al. 2012a, 2013; Sugime et al. 2019). Intriguingly, two copies of *dac* occur in some arachnids like spiders, and it was previously shown that the two copies exhibit dissimilar expression domains during embryogenesis of two spider species (Turetzek et al. 2016). One copy, *dac-1*, retains the conserved medial expression domain characteristic of the *dac* single copy ortholog in other arthropods, whereas the second, *dac-2*, exhibits a proximal domain in the coxa and body wall, as well as a novel, more distal ring of expression in the presumptive patellar segment (Turetzek et al. 2016). Maternal RNA interference (RNAi) against *dac-2* in the spider *Parasteatoda tepidariorum* resulted in a loss of the patellar-tibial boundary and consequent fusion of these segments. This result was interpreted to mean that the origin of the patella was caused by neofunctionalization of the *dac-2* copy, as *dac-2* was shown to be present at least in the common ancestor of spiders and scorpions (and by extension, across chelicerates). RNAi against *dac-1* was not reported in that work, and no functional data are available for *dac-1* in any spider species. As such, the inference of an ancestral function for *dac-1* (PD axis patterning in the medial segments) is based solely upon gene expression patterns in the two spider models (Turetzek et al. 2016).

On their own, these results certainly implicate *dac-2* as responsible for the origin of the patella. But this reconstruction is problematic for several, interconnected reasons, especially given recent advances in chelicerate genomics. First, *dac-2* is not common to all arachnids, but rather, restricted only to a subdivision of chelicerate orders called Arachnopulmonata, which are united by a shared whole-genome duplication (which is thought to have given rise to *dac-2*; Nolan et al. 2020) (fig. 1*b*). Many lineages of apulmonate arachnids (e.g. Opiliones, Ricinulei) that diverged prior to this genome duplication event have only a single copy of *dac*, but putatively possess a patella. Thus, *dac-2* is significantly younger than the origin of this novel podomere. In typical cases of derived traits arising from neofunctionalization, the new trait occurs either phylogenetically coincident with, or subsequent to, the appearance of the new gene that facilitates its expression. Notably, several copies of *dac* also occur in Xiphosura, but these are unrelated to the arachnopulmonate duplication as Xiphosura has experienced three rounds of comparatively recent and lineage-specific whole genome duplication (Nong et al. 2021). Thus, though Xiphosura also possess patellae, they do not possess an ortholog of spider *dac-2*. These patterns suggest that the origin of the patella is older than, and therefore not a consequence of, *dac-2* origin.

Second, a clear definition of the patella is elusive, and its presence is controversial in various chelicerate orders (fig. 2; supplementary tables S1 and S2, Supplementary Material online). Traditionally, the patella has been contextually defined as the small, compact podomere falling between the larger femur and tibia; it is therefore the fourth podomere of the chelicerate walking leg. Scorpions, however, possess an elongate patella that can exceed the size of the more distal tibia and creates the prominent rectangular bend characteristic of their walking legs (fig. 2h). The fourth podomere of pseudoscorpion appendages is likewise elongated (fig. 2g). Historically, the putative homology of this podomere was subject of much debate with several prominent works refuting presence of the patella throughout the order, instead

Downloaded from https://academic.oup.com/mbe/article/41/9/msae188/7749772 by guest on 11 October 2024

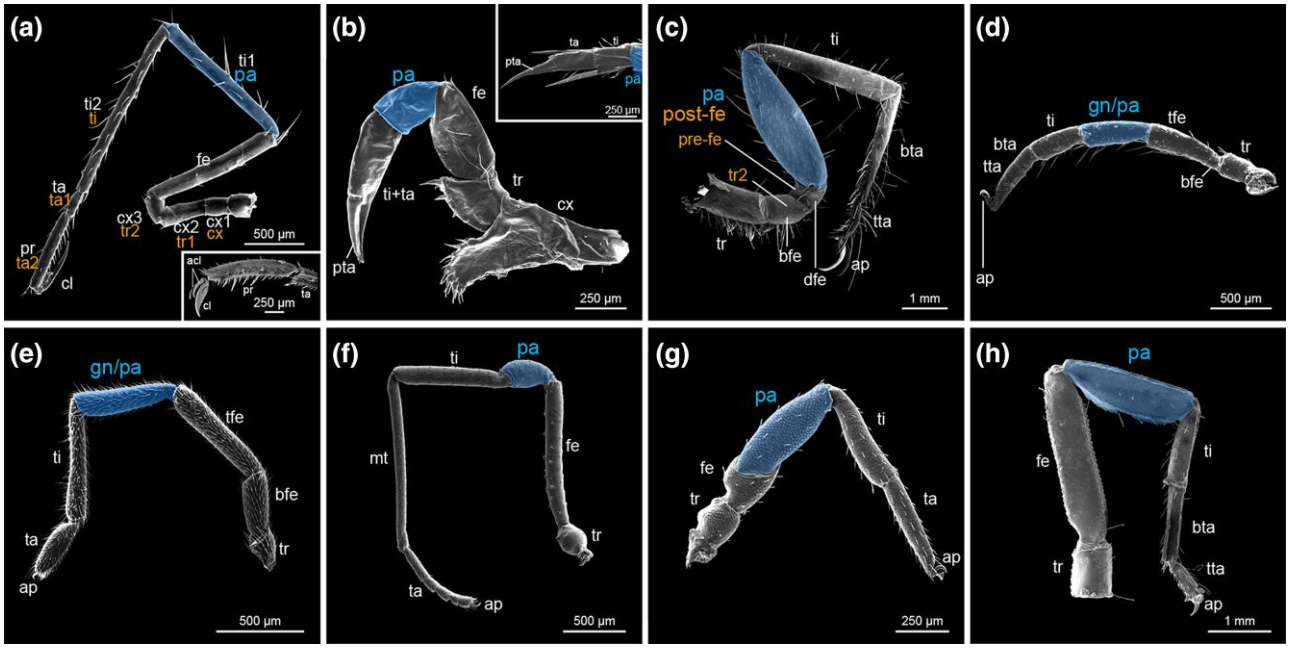

Fig. 2. The patella is inconsistently defined across Chelicerata. (**a–h**) Scanning electron micrographs (SEMs) of legs for selected orders. (**a**) Leg four of sea spider *Nymphon* sp. (Pycnogonida). Inset: distal podomere morphology of *Nymphon gracile* leg. (**b**) Leg four of horseshoe crab *Limulus polyphemus* (Xiphosura). Inset: distal podomere morphology of the pusher leg (leg V). (**c**) Leg four of camel spider *Mummucia* sp. (Solifugae). (**d**) Leg four of tick *Ixodes scapularis* (Parasitiformes, Ixodida). (**e**) Leg one of velvet mite *Trombidium* sp. (Acariformes, Trombidiformes). (**f**) Leg three of harvestman *Zalmoxis furcifer* (Opiliones). (**g**) Leg one of pseudoscorpion *Pselaphochernes scorpioides* (Pseudoscorpiones). (**h**) Leg one of scorpion *Scorpio palmatus* (Scorpiones). Blue shading: putative patellar homologs. White and orange text indicate alternative nomenclature. Abbreviations: acl: auxiliary claw; cx, coxa; tr, trochanter; fe, femur; bfe, basifemur; tfe, telofemur; dfe, distifemur; pa, patella; gn, genu; ti, tibia; mt, metatarsus; ta, tarsus; bta, basitarsus; tta, telotarsus; pr, propodus; cl, claw; pta, pretarsus; ap, apotele.

opting to term it a bipartite femur (e.g. Savory 1964), while others argued for its presence as a synapomorphy of Arachnida (e.g. Snodgrass 1958). Yet, convergent fusions across pseudoscorpion families between metatarsus and tarsus, as well as between both segments of the bipartite femur, confounded consistent alignment of their podomeres with other arachnid orders. More recent works, however, have routinely defined the fourth podomere of pseudoscorpions as the patella, irrespective of podomere size (Shultz 1989; Harvey 1992; Michalski et al. 2022).

Exacerbating this confusion, the phylogenetic placement of Pseudoscorpiones had long been unstable. Pseudoscorpions were initially thought to be closely related to Solifugae (camel spiders), which similarly lack an obvious patellar segment but clearly possess a metatarsus. The putative shared absence of a patella had thus been historically leveraged as one of several morphological characters uniting Pseudoscorpiones and Solifugae in the clade Apatellata (Haplocnemata) (van der Hammen 1977, 1985, 1986), though this relationship has never been recovered by analyses of molecular sequence data (e.g. Regier et al. 2010; Sharma et al. 2014; Ballesteros and Sharma 2019; Ballesteros et al. 2022). Likewise, Solifugae have historically demonstrated an unstable phylogenetic position across molecular analyses (Regier et al. 2010; Sharma et al. 2014; Ballesteros and Sharma 2019; Ballesteros et al. 2019, 2022). However, recent sequencing efforts to produce the first embryonic transcriptomes of both Pseudoscorpiones and Solifugae refuted the Apatellata hypothesis on the basis of a shared whole genome duplication between pseudoscorpions and the remaining arachnopulmonates, to the exclusion of Solifugae (Ontano et al. 2021; Gainett et al. 2024b) (Fig. 1b).

At present, although a sister group relationship between the two orders has been overturned, debate persists over the homology of their podomeres. An additional podomere is found in the third and fourth walking legs of solifuges, as well as subsets of walking legs in groups like Ricinulei (hooded tick spiders), Trigonotarbida (extinct), and some Eurypterida (extinct) (Shultz 1989), but many workers consider this segment to be homologous to the more distal segment of a bipartite femur (i.e. basifemur and distifemur; Punzo 1998). Many other chelicerate orders exhibit discordant leg segment alignments, each with their own lineage-specific nuances. The segmental homologies of Acariformes (mites) and Parasitiformes (mites and ticks; together forming the likely polyphyletic Acari) are likewise obscured. As in pseudoscorpions, many groups of acariform mites possess a subdivision of the femur forming basi- and telofemora, the latter of which therefore represents the fourth podomere of their walking legs. The adjacent segment, rather than patella, is instead referred to as the genu. However, this terminology was largely adopted subsequent to the early work of A.D. Michael on British oribatid mites, which themselves possess a secondary fusion of both femora in all but the

Downloaded from https://academic.oup.com/mbe/article/41/9/msae188/7749772 by guest on 11 October 2024

most early-diverging families (Michael 1884), synthesizing alternative terms such as *la jambe* (Dugès 1834), femur (Fumouze and Robin 1867), or 1st article (Donnadieu 1875), and use of genu by earlier authors (Nicolet 1855). The alignment of genu and patella in the fourth podomere of Oribatida and many other arachnid orders had thus been supposed to reflect homology and select authors have since used the terms interchangeably in both taxonomic and comparative arachnological works (e.g. Shultz 1989; Evans 1992; Harvey 1998; Krantz et al. 2009). Similarly, parasitiform mites and ticks also possess a genu segment and largely retain ancestral basi- and telofemora (Krantz et al. 2009). Opilioacaridae, the putative sister group to the remaining Parasitiformes, present additional subdivision of the trochanter (basi-, telotrochanter), although patterns of segment innervations suggest the subdivision is superficial (van der Hammen 1970).

These patterns of segment gain and loss across chelicerate orders undermine definitions for the patella that are based upon either position or shape. Inferring the origin of the patella is further stymied by leg architecture in Pycnogonida, the sister group of the remaining chelicerates. In sea spiders, numerous historical and primarily descriptive works have failed to converge on a consistent terminology for the pycnogonid podomeres, complicating interpretations of segmental homology. All studies on extant species report the presence of eight podomeres (when not including the distal claw), but most sea spider workers infer the leg to consist of three coxae, a femur, two tibiae, and two distal segments (Hoek 1881; Sars 1891; Meinert 1899; Helfer and Schlottke 1935; King 1973; Arnaud and Bamber 1988; Brusca and Brusca 2003). Only a minority of works have inferred the fifth podomere to be the putative patellar segment (Snodgrass 1958; Dencker 1974; Schram and Hedgpeth 1978; Shultz 1989; Sabroux et al. 2023).

Thus, both the developmental genetic basis for the origin of this podomere, as well as its incidence across Chelicerata, is poorly understood. Breaking this impasse therefore requires the identification of a potential genetic mechanism underlying patella formation that is phylogenetically consistent with the age of the trait, and that can also be surveyed across chelicerate taxa to test for the presence of a patella. Of the four transcription factors required for the establishment of the arthropod PD axis (Dong et al. 2001), the arachnid homolog of *extradenticle* (*exd*) exhibits both ancestral and novel expression domains. Shared with other arthropods, arachnid *exd* has a conserved proximal domain (overlapping with *homothorax* expression; the two genes operate as a heterodimer to pattern proximal leg segments). Additionally, arachnid *exd* has a novel distal ring of expression in the presumptive patella. This distal expression domain is observed in both the single copy ortholog of *exd* in the harvestman *Phalangium opilio* (Sharma et al. 2012a), as well as *exd* paralogs of spiders and scorpions (Pechmann and Prpic 2009; Nolan et al. 2020), but its function is not known.

Here, we show that this distal ring domain of *exd* is required for patterning the patella-tibia boundary of the harvestman *Phalangium opilio*. Disruption of Notch signaling results in diminution of this distal *exd* domain, supporting the interpretation that it plays a role in segmentation. Armed with a developmental genetic definition of patellar identity, we survey exemplars of chelicerate diversity and demonstrate that a patella homolog is present in phylogenetically significant chelicerate groups, such as sea spiders, mites, and pseudoscorpions. These results suggest that a patella was present in the common ancestor of Chelicerata.

Results

A Distal Domain of *exd* Abuts the Patella-Tibia Boundary During *P. opilio* Embryonic Appendage Development

In early outgrowth of the limb bud (stage 9; stages following Gainett et al. [2022]), *Po-dac* is expressed in a medial territory proximal to the expression domain of *Po-Distal-less* (*Po-Dll*) (fig. 3*a*; supplementary fig. S1 to S3, Supplementary Material online). At this early stage, *Po-exd* is detected as two discontinuous domains: one occurs proximally in the presumptive coxal segment and body wall, whereas a second ectodermal ring is observed distal to the *Po-dac* domain. Weak, diffuse *Po-exd* expression is also observed distal to the ring domain, into the tip of the appendage during this early stage. As the appendages elongate in later stages of development, the medial *Po-dac* domain and the distal *Po-exd* domain expand and become heterogeneous in expression intensity along the PD axis (fig. 3*b*–*d*; supplementary fig. S3, Supplementary Material online). By stage 10, the *Po-dac* domains exhibit two stronger rings of expression that correspond to the presumptive distal trochanter and the distal femur, with weaker expression signal between these domains (fig. 3*b*; supplementary fig. S3, Supplementary Material online). Subsequent resolution of these domains in stage 11 and stage 12 embryos yields stronger localization in the distal femur and trochanter territories, as well as a third ring domain in the distal coxa (fig. 3*c* and *d*; supplementary fig. S3, Supplementary Material online). The restricted expression of *Po-dac* in the medial territory of the developing appendage mirrors *dac* expression domains across other arthropod lineages, particularly insects, wherein *dac* loss-of-function mutants exhibit deletion of the femur and tibia (Angelini and Kaufman 2004; Sewell et al. 2008; Angelini et al. 2009, 2012).

In contrast to mandibulate development (e.g. insect; amphipod; millipede), a distal ring of *Po-exd* expression is detected early in the outgrowth of the limb bud (stage 9), with minimal overlap of expression with the more proximal *dac* domain (fig. 3*a*; supplementary fig. S3, Supplementary Material online). By stage 11, this domain encompasses nearly the entire patellar segment, whereas the weaker, more distal expression spans the presumptive tibial segment (fig. 3*b* and *c*; supplementary fig. S3, Supplementary Material online). In stage 12 embryos, the strong *Po-exd* domain abuts the

Downloaded from https://academic.oup.com/mbe/article/41/9/msae188/7749772 by guest on 11 October 2024

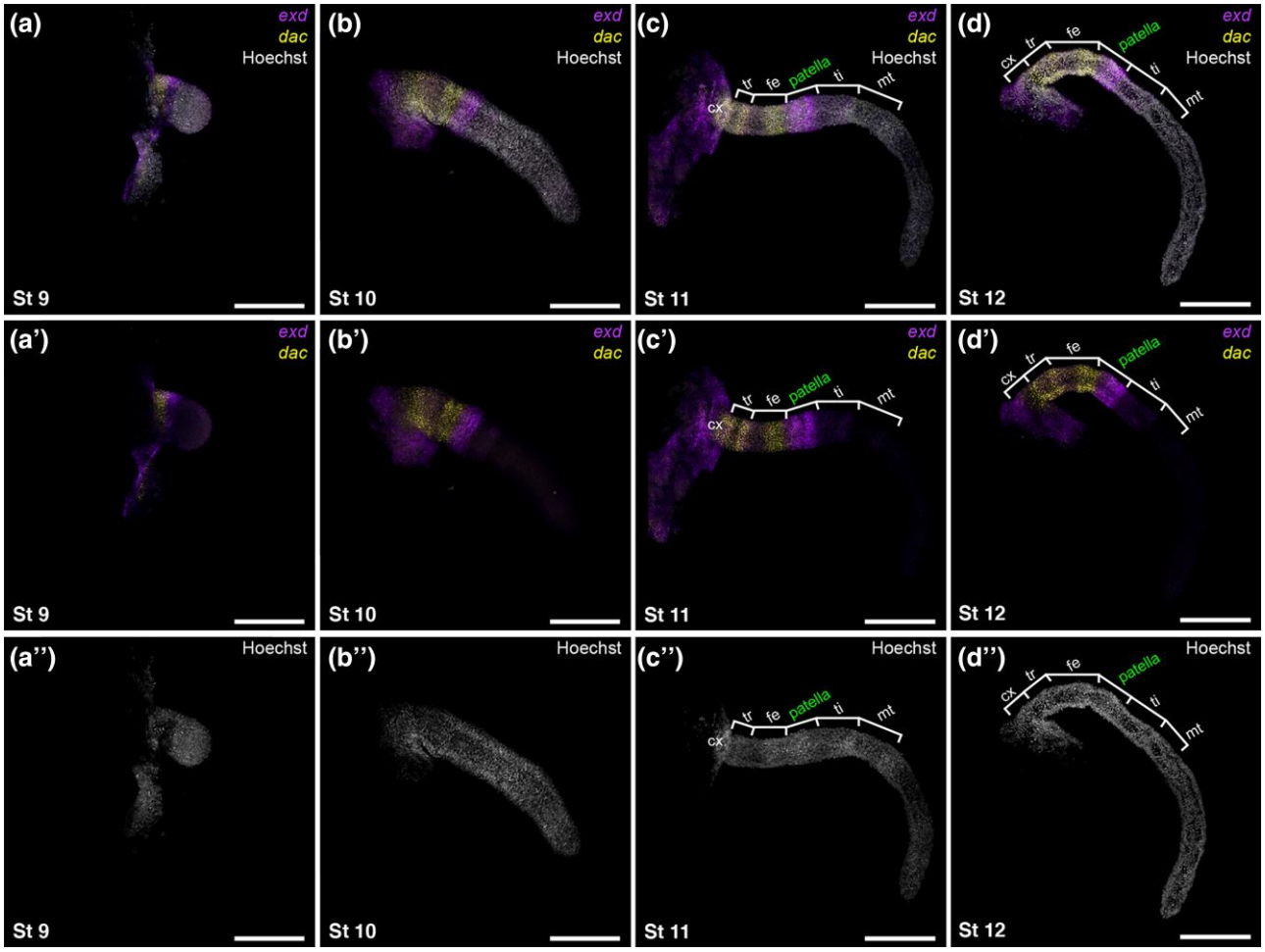

Fig. 3. A distal ring domain of *Po-exd* is established early in *P. opilio* embryonic development and localizes to the patella-tibia segmental boundary. (**a–d**) Leg mounts of L2 in selected stages with merged visualization of Hoechst counterstaining (white), *Po-exd* (magenta), and *Po-dac* (yellow). (**a′–d′**) Multiplexed expression of *Po-exd* and *Po-dac*. (**a″–d″**) Isolated Hoechst counterstaining. Abbreviations: cx, coxa; tr, trochanter; ti, tibia; mt, metatarsus. Scale bars: 250 µm.

patella-tibia boundary, whereas the more proximal patellar territory experiences a slight gradation of weakening expression and slight expansion of the *Po-dac* territory into the femur-patella boundary (fig. 3*d*; supplementary fig. S3, Supplementary Material online).

The Distal Domain of *Po-exd* is Necessary for Establishing the Distal Boundary of the Patella

To assess the function of *Po-exd* in developing appendages, we performed embryonic RNAi via microinjection of double-stranded RNA (dsRNA) against *Po-exd* at two different points during *P. opilio* development (fig. 4). Embryos were injected at either stage five (early germband; henceforth, "early knockdown") or stage seven (initial formation of prosomal limb buds; henceforth, "late knockdown"). Early knockdown of *Po-exd* incurred an array of major developmental defects that spanned irregular development of the head and failure to form the ocularium (prosomal protrusion bearing the median eyes); defects of antero-posterior segmentation and truncation of posterior segments; and segmental fusions (fig. 4*a–e*; supplementary fig. S4, Supplementary Material online). Segmental defects of the prosoma included asymmetric fusions of adjacent segments and irregular placement of appendages, which exhibited proximal truncations (fig. 4*d* and *e*). Embryos exhibiting this array of phenotypes did not survive to hatching, necessitating manual dissection from vitelline membranes for subsequent imaging. These loss-of-function phenotypes closely parallel known phenotypic spectra for *exd* loss-of-function experiments in mandibulate arthropods, suggesting that the function of *exd* is conserved across arthropods with respect to early development (Rauskolb et al. 1995; Mito et al. 2008; Bruce and Patel 2020). Abnormal morphogenesis, including aberrant appendage localization without homeotic transformations, is consistent with previous studies demonstrating that Hox genes require nuclear Exd and Hth proteins as cofactors for proper specification of the body wall, while Hox transcription factors operate independently to specify appendage identity (Smith and Jockusch 2014). Likewise, appendage truncations are consistent with independent *exd* and *hth* specification of proximal appendage identity (Smith and Jockusch 2014).

Downloaded from https://academic.oup.com/mbe/article/41/9/msae188/7749772 by guest on 11 October 2024

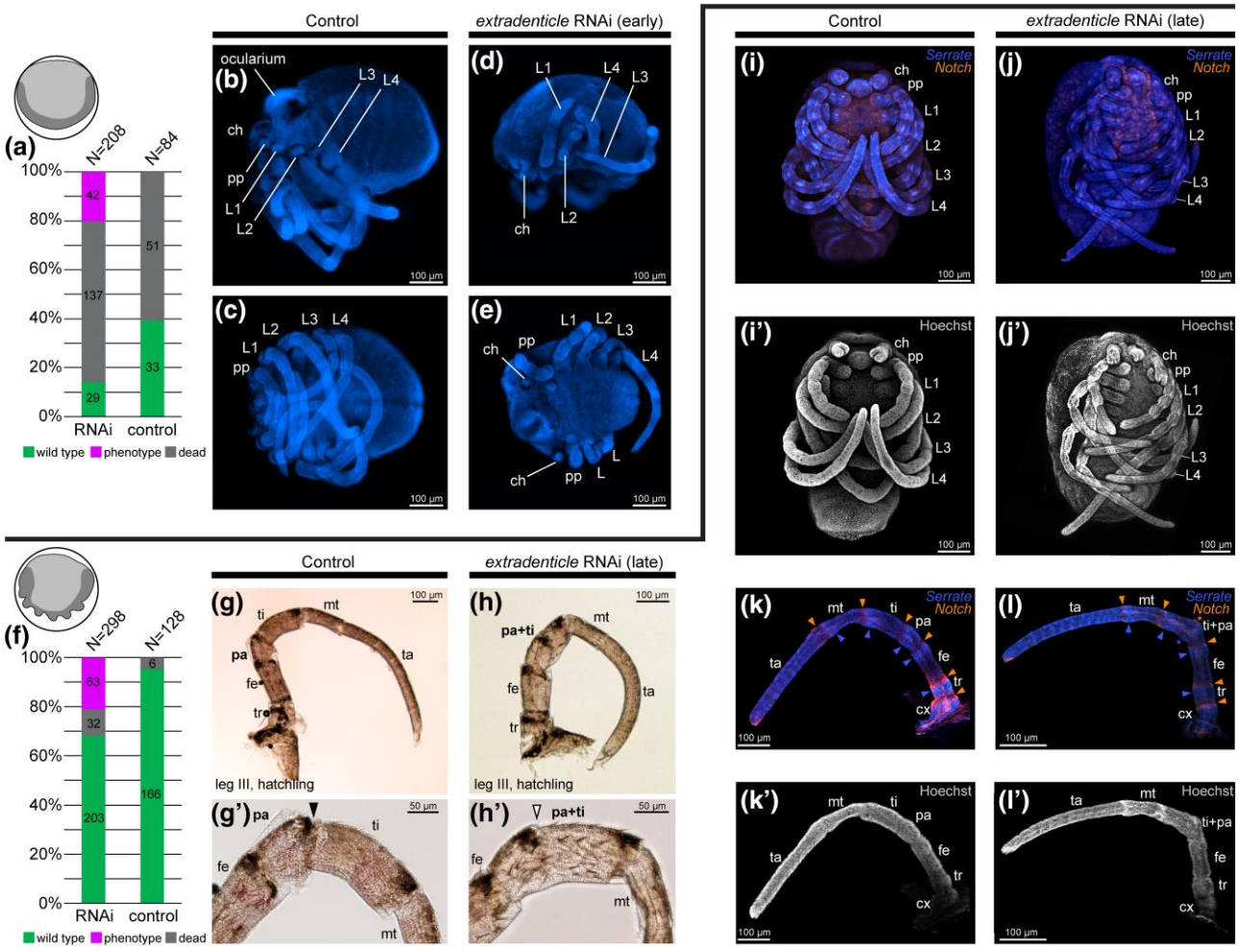

Fig. 4. RNAi against *Po-exd* incurs a fusion at the patella-tibia joint in *P. opilio*. Icons indicate morphology of early and late RNAi embryos. Dark grey corresponds to the germband. (**a**) Distribution of outcomes following early *Po-exd* RNAi or negative control injections. Embryos were scored as dead only if they exhibited no further development following RNAi microinjection. (**b**–**e**) Hoechst staining of late stage embryos for early knockdown. (**b**) Negative control embryo, lateral view. (**c**) Same embryo as in (**b**), ventral view. (**d**) *Po-exd* RNAi embryo, lateral view. (**e**) *Po-exd* RNAi embryo, ventral view. Note posterior truncation and proximal leg defects in RNAi embryos. (**f**) Distribution of outcomes following late *Po-exd* RNAi or negative control injections. (**g**–**l′**) Late knockdown of *Po-exd*. (**g**) Leg three of negative control hatchling. (**g′**) Same hatchling as in (**g**), showing magnification of patella-tibia joint. (**h**) Leg three of *Po-exd* RNAi hatchling exhibiting fusion of patella-tibia joint. Note the location of melanized cuticle at dorso-distal boundary of femur, patella, and tibia. (**h′**) Same hatchling as in (**h**), showing magnification of fused patella-tibia joint. Black arrowhead: wild type patella-tibia joint. White arrowhead: fused patella-tibia joint. (**i**) Negative control embryo with expression of *Po-Serrate* (blue) and *Po-Notch* (orange). (**i′**) Same embryo as in (**i**) with Hoechst nuclear counterstaining. (**j**) Late *Po-exd* RNAi embryo with expression of *Po-Ser* and *Po-N*. (**j′**) Same embryo as in (**j**) with nuclear counterstaining. (**k**) Leg four of negative control embryo with expression of *Po-Ser* and *Po-N*. Note strong expression of *Po-Ser* and *Po-N* in the distal and proximal compartments of each podomere, respectively. (**k′**) Same appendage as in (**k**) with nuclear counterstaining. (**l**) Leg four of late *Po-exd* RNAi embryo with expression of *Po-Ser* and *Po-N*. Note disrupted expression of *Po-Ser* and *Po-N* in the fused tibia and patella. (**l′**) Same appendage as in (**l**) with nuclear counterstaining. Orange arrowheads: ring domains of *Po-N* in the proximal territory of developing podomeres. Blue arrowheads: ring domains of *Po-Ser* in the distal territory of developing podomeres. Asterisks: disrupted *Po-Ser* and *Po-N* at the fused boundary of tibia and patella. Abbreviations: ch, chelicera; pp, pedipalp; L1, leg one; L2, leg two; L3, leg three; L4, leg four; sp, spiracle; O2, second opisthosomal segment; cx, coxa; tr, trochanter; fe, femur; pa, patella, ti, tibia; mt, metatarsus; ta, tarsus.

The effects of early *Po-exd* knockdown on the appendages precluded assessment of its role in specification of the patellar boundary. We therefore performed late knockdowns to interfere with *Po-exd* expression in stages where prosomal segmentation and body wall patterning had been established (Gainett et al. 2022) (fig. 4*f*–*h*). Late knockdown of *Po-exd* resulted in embryos that were largely wild type in morphology and able to complete hatching, but exhibited a fusion of the patella and tibia, as well as a shortening of the tibia (fig. 4h). The interpretation of a fusion of segments, rather than a deletion, is substantiated by the retention of melanized patches at the distal and dorsal termini of the femur, patella, and tibia in hatchlings (fig. 4h′).

To validate the interpretation of patella-tibia fusion resulting from a segmentation defect, we assayed both negative control and late *Po-exd* RNAi embryos for expression of *Po-Notch* (*Po-N*) and *Po-Serrate* (*Po-Ser*) (fig. 4*i*–*l′*). In

Downloaded from https://academic.oup.com/mbe/article/41/9/msae188/7749772 by guest on 11 October 2024

spider models, both *N* and *Ser* are initially ubiquitously expressed in developing appendages at early stages, later resolving into a series of ring domains at the boundaries of each podomere (Prpic and Damen 2009). Disruption of either gene's expression in the spider resulted in appendages with a wrinkled, disorganized appearance and a complete lack of podomere formation (Prpic and Damen 2009). In the appendages of *P. opilio* controls, *Po-N* and *Po-Ser* were detected in adjacent, non-overlapping domains at the distal boundary of each podomere (fig. 4*k*). However, late *Po-exd* RNAi appendages demonstrating the fusion phenotype failed to form the ring domains of both *Po-N* and *Po-Ser* at the presumptive patella-tibia boundary, while ring domains remained present at the boundaries of all other podomeres (fig. 4*l*). Cumulatively, these results suggest that the distal ring of *Po-exd* is required to form the distal segmental boundary of the patella.

The Distal Domain of *Po-exd* is Regulated by Notch Signaling

The distribution of *Po-exd* transcripts during patella formation is reminiscent of the ring domains characteristic of leg segmentation genes in the Notch-Delta signaling pathway in both spider and insect model systems, such as *Delta*, *Serrate*, and *nubbin* (Rauskolb and Irvine 1999; Prpic and Damen 2009). To test whether the distal domain of *Po-exd* is under the control of the Notch signaling cascade, we performed late knockdown of *Po-Notch* (*Po-N*). The later delivery of dsRNA was selected to minimize early developmental defects that would impair appendage outgrowth.

Po-N RNAi embryos were broadly characterized by prominent segmental and neurogenic phenotypes (fig. 5; supplementary fig. S5 and S6, Supplementary Material online). Embryos exhibiting such phenotypes did not survive to hatching, again necessitating manual dissection from vitelline membranes. As compared to the small, uniformly distributed rosettes of invaginating cells in the ventral neuroectoderm of wild type embryos, *Po-N* embryos instead demonstrate large, irregular pockets of cells, consistent with failed invagination of the neuroectoderm (fig. 5*b*; supplementary fig. S5b, S6, Supplementary Material online). This outcome reflects a previously reported *Notch* RNAi phenotype in the spider *Cupiennius salei* (Stollewerk 2002), which resulted in failed invagination and yielded an accumulation of cells in the apical layer of the ventral ectoderm. While Notch signaling mediates cell interactions within these neural clusters, *Notch* is also required for lateral inhibition of the territory surrounding these clusters, limiting their size via activation of the *split* gene complex that represses neural identity (Chen et al. 2023). Consistent with this known activity, irregular development of the central nervous system could also be visualized via expression of *Po-dac*, which showed defects in developing segmental neuromeres (supplementary fig. S5b, Supplementary Material online). The appendages of *Po-N* RNAi embryos displayed reductions in length and a wrinkled appearance compared to wild type appendages, consistent with previously reported *Notch* phenotypes in *C. salei* (Prpic and Damen 2009). Uniquely, *Po-N* RNAi also yielded consistent defects in the distal-most territory of most appendages, appearing as either early bifurcation or a central lacuna of tissue. *Po-N* RNAi embryos also exhibited abnormal development of the labrum, resulting in a smaller and circular structure, as opposed to the subtriangular wild type counterpart.

To validate the incidence of segmental defects in *Po-N* RNAi embryos, we assayed expression of the segment polarity gene *engrailed* (*en*) (fig. 5; supplementary fig. S6, Supplementary Material online). In wildtype embryos, *Po-en* was expressed in broad stripes in the posterior compartment of each segment. Expression was also detected in the posterior portion of each appendage along the length of the PD axis. Weak phenotypes in *Po-N* RNAi experiments retained *Po-en* expression in each body segment, but expression was more diffuse and remained localized near the ventral midline (supplementary fig. S6b, Supplementary Material online). In the appendages, the strongest *Po-en* expression was found in small territories at the distal terminus, yet subsets of appendages still showed weak expression throughout the PD axis. In severe phenotypes, *Po-en* was not detected in the ventral ectoderm, and only the distal tip expression is detectable in appendages (supplementary fig. S6c, Supplementary Material online). These results corroborate previous segmentation defects and aberrant deployment of segment polarity genes following abrogation of Notch signaling in arachnid and mandibulate embryos (Stollewerk et al. 2003; Pueyo et al. 2008; Eriksson et al. 2013).

To test the regulatory relationship of *Po-N* and the distal ring of *Po-exd*, we assayed *Po-N* RNAi embryos for expression of limb patterning genes. In *Po-N* RNAi embryos, expression of *Po-dac* in the medial territory is retained, but reduced (supplementary fig. S5b, S7, Supplementary Material online). Similarly, abrogation of *Po-N* resulted in marked diminution of *Po-exd* throughout the appendages, consistent with the interpretation that appendicular *Po-exd* expression is regulated by the Notch segmentation cascade (fig. 5*b″*; supplementary fig. S5*b″*, S7*b*, Supplementary Material online). These results partially reflect a previous experiment in the spider *C. salei*, wherein RNAi against the spider *Notch* homolog resulted in abrogation of the distal ring of *exd-1*, but had no effect on the expression of *dac*, *Dll*, or the proximal domain of *exd* (Prpic and Damen 2009). It was previously suggested that the distal *exd-1* domain could be uniquely operating downstream of Notch signaling, but since that work, the function of *exd-1* has not been investigated to date in any spider.

Taken together, these results support the interpretation that a distal, arachnid-specific expression domain of *exd* has acquired a novel segmentation function responsible for patterning the patella-tibia boundary.

Po-dac Plays a Role in Segmentation After Appendage Outgrowth

The coincidence of loss-of-function phenotypes in the spider *dac-2* and *Po-exd* experiments impels a reappraisal of the evolutionary role of *dac* in appendage patterning. In insects, *dac* is known to be required for leg morphogenesis

Downloaded from https://academic.oup.com/mbe/article/41/9/msae188/7749772 by guest on 11 October 2024

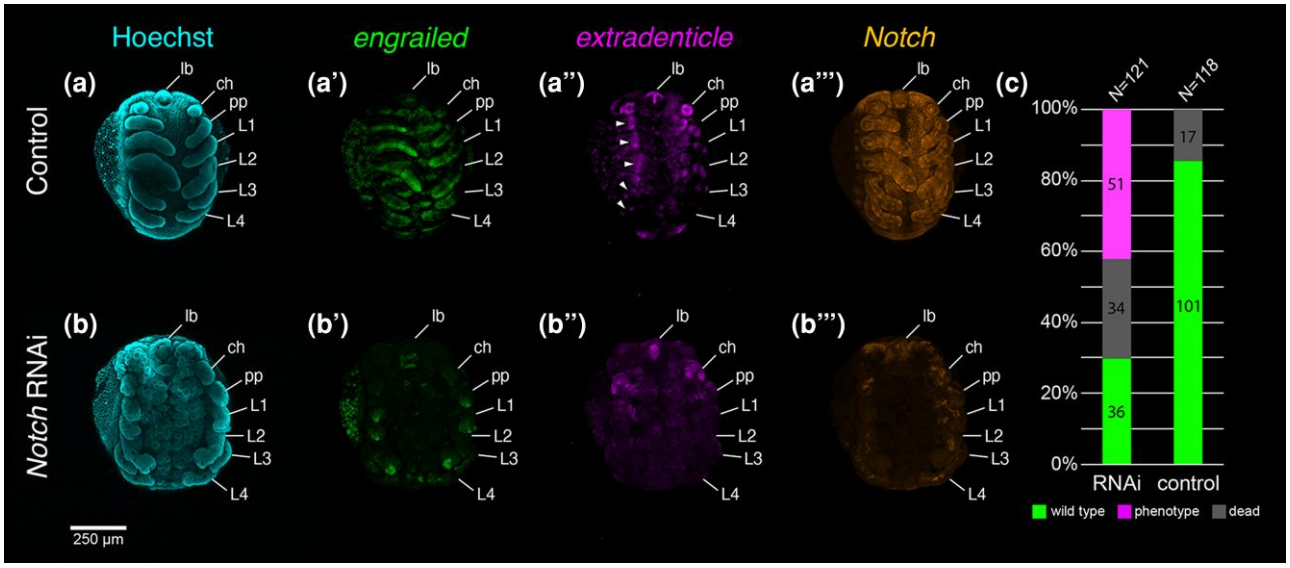

Fig. 5. Knockdown of *Po-N* yields broad developmental defects and diminution of the *Po-exd* distal ring domain. (**a**) Stage 10 negative control embryo in ventral view with Hoechst counterstaining (cyan). (**a′**–**a‴**) Same embryo as in (**a**) with expression of *Po-en* (green, **a′**), *Po-exd* (magenta, **a″**), and *Po-N* (orange, **a‴**). (**b**) Stage 10 *Po-N* RNAi embryo with Hoechst counterstaining. (**b′**–**b‴**) Same embryo as in (**b**) with expression of *Po-en* (**b′**), *Po-exd* (**b″**), and *Po-N* (**b‴**). (**c**) Distribution of outcomes following *Po-N* RNAi or negative control injection. White arrowheads: distal ring domains of *Po-exd* in wild type embryo. Abbreviations: lb, labrum; ch, chelicera; pp, pedipalp; L1, leg one; L2, leg two; L3, leg three; L4, leg four.

and elongation of the medial appendage territory (Mardon et al. 1994). Nevertheless, in later development, *dac* is known to be required for the patterning of insect podomere boundaries and is required for establishing the segmentation pattern of *Notch* and *fringe* in the developing fruit fly leg (Dong et al. 2001; Rauskolb 2001). One possible interpretation of the spider *dac-2* segmentation phenotype is that, rather than reflecting a derived trait, the loss of the distal patellar boundary reflects a more ancient role of *dac* in patterning the segmental boundaries of this territory, a function already present in single-copy *dac* homologs across Panarthropoda. A previous investigation of *dac* function in *P. opilio* yielded a canonical limb gap phenotype, with deletions of the femur and patella in the leg and palp, as well as the proximal segment of the chelicera, precluding a test of this hypothesis (Sharma et al. 2013). We reasoned that *dac* may continue to play a role in regulating limb segmentation following outgrowth of these segments after their specification, a function that could be examined by interfering with *dac* expression later in development.

To test this reasoning, we performed early and late knockdown of *Po-dac*, following the same experimental strategy as for *Po-exd* (fig. 6). Early knockdown of *Po-dac* recapitulated the result of a previous experiment (fig. 6*c* and *d*). Late knockdown of *Po-dac* incurred a milder phenotypic spectrum, characterized by shortening and/or fusion of medial segments of the palps and legs, but no defects of proximal (coxa and trochanter) or distal (metatarsus and tarsus) segments (fig. 6*e*–*g*). Fusions were interpretable based on pigmentation patterns of medial podomeres. The most severe condition observed in late knockdown embryos consisted of fusion of the trochanter through the tibia (fig. 6*g*). Notably, late knockdown *Po-dac* embryos exhibited a visibly shorter and thickened medial palp and leg territory, consistent with the phenotype described for hatchlings from this experiment (fig. 7). Despite modest reduction of *Po-dac* expression, the spatial arrangement of *Po-dac* and the distal *Po-exd* domain was not altered, and the distal ring of *Po-exd* in the palps and legs was not visibly affected (fig. 7*b* and *c*). These results are consistent with a role for *dac* in regulating podomere segmentation in medial leg segments after limb bud outgrowth. This outcome also disfavors the interpretation that the patella boundary-forming function of spider *dac-2* represents a novel function.

Limb Patterning Gene Expression Dynamics in the Sea Spider *Pycnogonum litorale*

In contrast to arachnids, most sea spiders undergo pronounced indirect development, characterized by the hatching of a protonymphon larva with three larval limb pairs only, which correspond to the chelicera, the pedipalp, and the oviger (supplementary fig. S8a, Supplementary Material online) (Vilpoux and Waloszek 2003; Brenneis et al. 2017). During postembryonic development, body segments bearing leg pairs form sequentially at the posterior terminus. Each of the four legs undergoes a similar sequence of developmental stages. Therefore, we primarily focused on leg 1 in instars II to IV.

The primordium of leg 1 is first discernible in late instar II (supplementary fig. S8a, Supplementary Material online). Distally, it displays *Pl-Dll* expression, which is proximally bordered by a narrow ring-like *Pl-dac* territory. A few *Pl-dac*-positive cells are located in the distal limb bud tip. The entire primordial bud expresses *Pl-exd* at low levels. A ring-like domain with stronger signal intensity partially

Downloaded from https://academic.oup.com/mbe/article/41/9/msae188/7749772 by guest on 11 October 2024

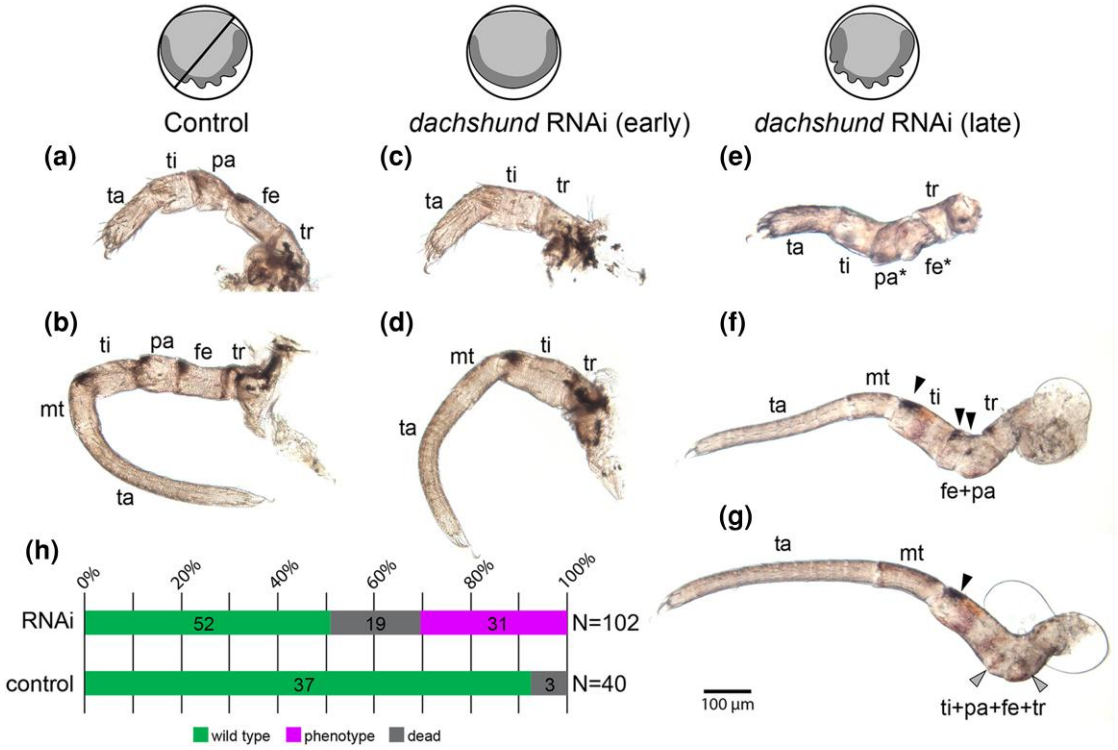

Fig. 6. Late RNAi against *Po-dac* results in segmental fusions of medial podomeres. Icons indicate early and late RNAi embryos. Dark grey corresponds to the germband. (**a**) Pedipalp of negative control hatchling. (**b**) Leg three of negative control hatchling. (**c**) Pedipalp of early knockdown hatchling. (**d**) Leg three of early knockdown hatchling. (**e**) Pedipalp of late knockdown hatchling. (**f**) Leg three of late knockdown hatchling. (**g**) Leg four of late knockdown hatchling. (**h**) Distribution of outcomes following late *Po-dac* RNAi or negative control injection. Black arrowheads: melanized cuticle patches at dorso-distal boundary of femur, patella, and tibia. Grey arrowheads: traces of melanized patches in knockdown phenotypes. Asterisks indicate segments with aberrant morphology.

overlaps with the *Pl-dac* ring and extends slightly further distally (supplementary fig. S8a, Supplementary Material online). In early instar III, leg 1 resembles a proper limb bud that projects posteriorly (fig. 8*a*; supplementary S8b, Supplementary Material online). *Pl-Dll* is still strongly expressed in the distal tip, showing a gradual decrease of intensity toward the medial limb bud portion. The ring-like *Pl-dac* territory is more pronounced than in the preceding instar, its distal boundary overlapping slightly with the *Pl-Dll* domain. In the limb bud's tip, the *Pl-dac*-positive cells persist. *Pl-exd* expression reaches from the bud's proximal base up to half of its length, being strongest along its distalmost portion that extends beyond the distal border of the *Pl-dac* territory (fig. 8*a*).

In advanced stages of instar III, the tissues of leg 1 have considerably expanded along the PD axis, but remain confined under the limb bud's rigid cuticle. This leads to a telescope-like folding and partial coiling of the leg tissue along the PD axis (fig. 8*b*; supplementary fig. S8c, Supplementary Material online). Spatial relationships of the gene expression domains remain unchanged, with *Pl-exd* featuring a ring-like territory distal to the *Pl-dac* ring. Furthermore, the distal *Pl-Dll* domain includes scattered clusters with higher expression levels (fig. 8*b*).

With the molt toward instar IV, leg 1 becomes functional and is comprised of six podomeres (fig. 8*c*) (Sánchez and López-González 2010; Brenneis et al. 2017). At this point, observed gene expression domains can be unequivocally assigned to discrete podomeres. Directly after the molt, the expression signal for all three genes was observed to be relatively weak, presumably due to the considerable stretching of the largely single-layered ectodermal cell layer, concomitant with the rapid leg extension (supplementary fig. S8d, Supplementary Material online). In mid- and late-stage instars IV, signal strength was observed to increase again (fig. 8*c*; supplementary fig. S8e, Supplementary Material online). *Pl-Dll* is strongly expressed in the main claw and the tarsus-propodus precursor. In the more proximal podomeres, scattered domains of stronger expression are primarily located in tissue underlying cuticular sensilla, suggesting a potential role of *Pl-Dll* in sensory cells. *Pl-dac* expression demarcates a medial domain that includes coxa 3 and the proximal portion of the femur-tibia 1 precursor, its distal boundary marking the border of the two future podomeres (fig. 8*c*). More distally, *Pl-dac* is upregulated only in scattered single cells, which may represent sensory cells. *Pl-exd* displays low expression levels along the entire PD axis, but the proximal coxa 1 as well as the distal two thirds of the femur-tibia 1 precursor and the entire tibia 2 show elevated expression (fig. 8*c*). In the femur-tibia 1 precursor, the proximal expression boundary overlaps slightly with the distal boundary of the *Pl-dac* domain.

Downloaded from https://academic.oup.com/mbe/article/41/9/msae188/7749772 by guest on 11 October 2024

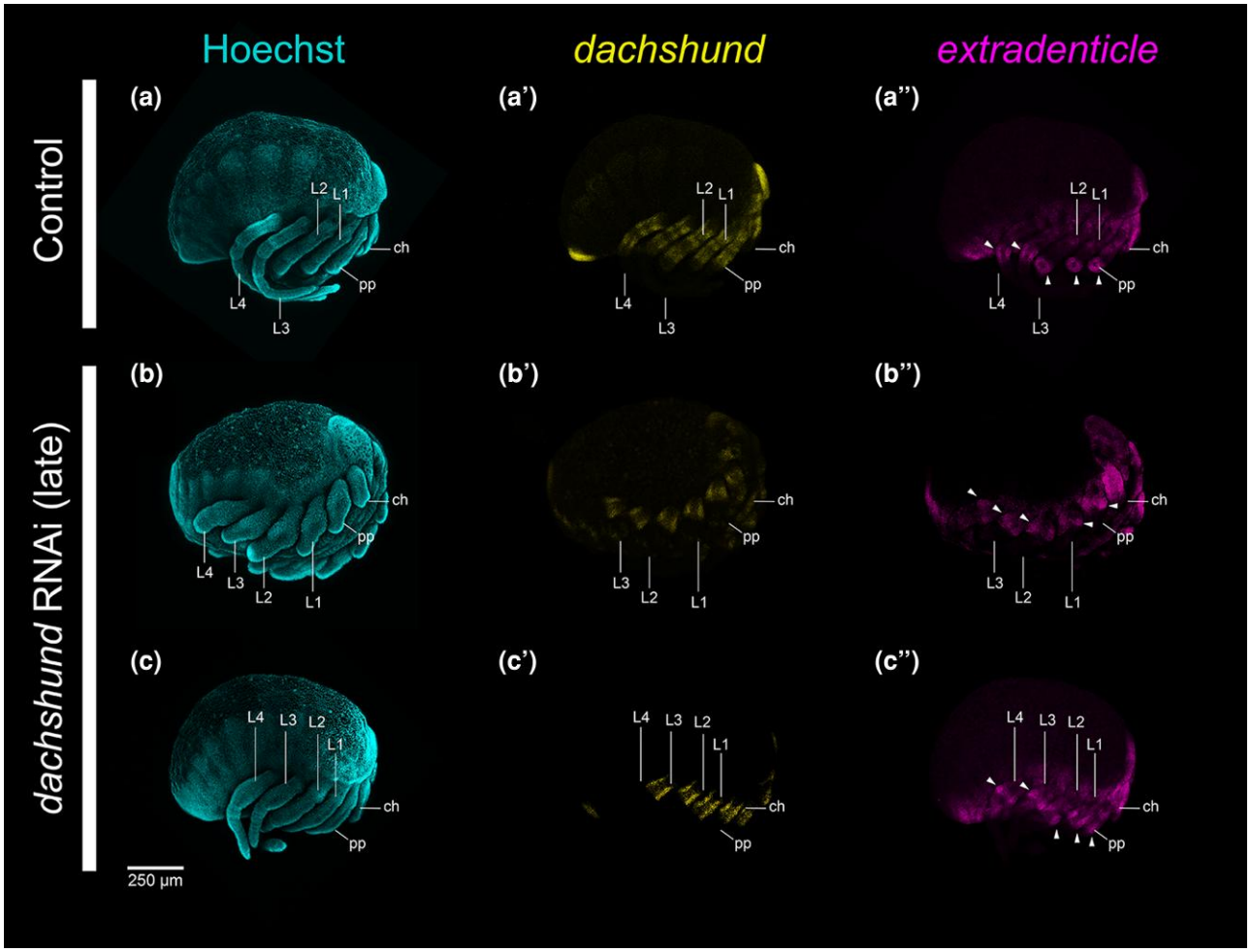

Fig. 7. Late RNAi against Po-dac does not diminish distal expression of *Po-exd*. (**a**) Negative control embryo in lateral view, with Hoechst counterstaining (cyan). (**a**′–**a**″) Same embryo as in (**a**) with single-channel expression of *Po-dac* (yellow, **a**′) and *Po-exd* (magenta, **a**″). (**b**–**c**″) *Po-dac* RNAi embryos in lateral view with Hoechst counterstaining (**b**, **c**), *Po-dac* expression (**b**′, **c**′), and *Po-exd* expression (**b**″, **c**″). Note the more severe medial appendage defects in (**b**) coincident with pronounced developmental delay. White arrowheads: distal ring domains of *Po-exd* expression in all embryos examined. Abbreviations: ch, chelicera; pp, pedipalp; L1, leg one; L2, leg two; L3, leg three; L4, leg four.

In the early stages of leg 2 and leg 3 development included in our experimental series, spatial relationships of gene expression correspond well to leg 1, with the additional observation that *dac* is the last of the three genes surveyed to be expressed in the earliest recognizable limb bud primordia (fig. 8; supplementary fig. S8b–S8e, Supplementary Material online). Taken together, the consistent expression of *Pl-exd* distal to the medial *Pl-dac* territory during *P. litorale* leg development closely mirrors the situation in *P. opilio*. Beyond this, the specific *Pl-dac* and *Pl-exd* expression domains in the segmented leg of instar IV provides the first molecular developmental arguments for the homology of these pycnogonid leg podomeres with those of other chelicerates. This includes the identification of the sea spider tibia 1 as the homolog of the patella (strong *exd* domain in *P. opilio*; fig. 3*c*) and the sea spider tibia 2 as the homolog of the arachnid tibia (weak *exd* domain in *P. opilio*; fig. 3*c*). This accords as well with the RNAi phenotype in *P. opilio*, wherein the patella boundary is lost and the tibia is shortened (fig. 4*h*).

Limb Patterning Gene Expression Dynamics in Non-Model Arachnids

We next examined the spatial relationships of *exd* and *dac* homologs in a subset of arachnid orders wherein the incidence of a patellar homolog has been historically disputed (fig. 9). In the developmental transcriptome of the pseudoscorpion *Pselaphochernes scorpioides*, we detected two copies of *exd* and *dac*, consistent with the recent placement of Pseudoscorpiones within Arachnopulmonata and the inference of a shared genome duplication (Ontano et al. 2021). In embryos of *P. scorpioides*, we detected expression domains of *dac* and *exd* homologs that largely reflected the patterns previously described for other arachnopulmonates (Prpic et al. 2003; Nolan et al. 2020). Expression of *Ps-dac-1* was observed in the femur and proximal patella of the palp and legs, whereas *Ps-exd-1* was observed as three domains: (a) a proximal domain corresponding to the body wall, coxa, trochanter, and proximal femur; (b) a median domain intercalating the *Ps-dac-1* expression domains at the femoro-patellar boundary; and (c) a distal domain

Downloaded from https://academic.oup.com/mbe/article/41/9/msae188/7749772 by guest on 11 October 2024

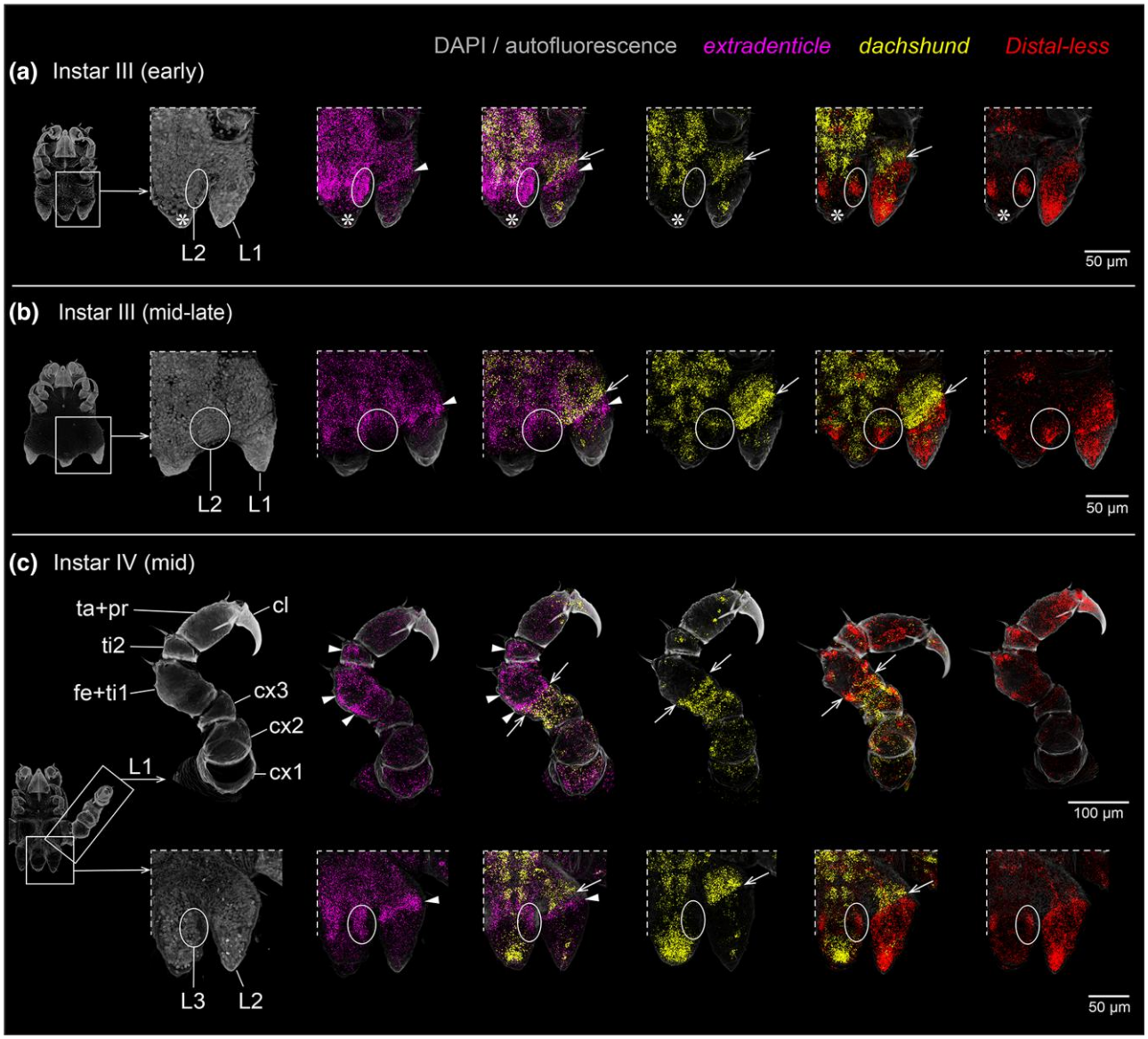

Fig. 8. *Pl-exd* is expressed in a ring-like domain distal to *Pl-dac* expression in the developing legs of the sea spider *P. litorale*. All images apart from upper row in (**c**) show a ventral detail of the posterior body pole as indicated to the left of each row. Arrows: distal boundary of *Pl-dac* domain. Arrowheads: *Pl-exd* expression distal to the *Pl-dac* domain. Ovals and circles: limb bud primordia hidden under the cuticle. Asterisks indicate region of damaged tissue at the tip of the posterior body pole. (**a**) Detail of leg 1 bud and leg 2 primordium in early instars III. (**b**) Detail of leg 1 bud and leg 2 primordium in mid- to late-stage instars III. (**c**) Upper row: dissected leg one of mid-stage instars IV. Lower row: detail of leg 2 bud and leg 3 primordium in mid-stage instar IV. Abbreviations: cx, coxa; fe + ti1, femur-tibia 1 precursor; L, leg; mc, main claw; ta + pro, tarsus-propodus precursor; ti2, tibia 2.

corresponding to the distal patella (fig. 9*a*). By contrast, the expression domains of *Ps-dac-2* and *Ps-exd-2* were more weakly detected in later developmental stages and comprised two overlapping rings at the femoro-patellar boundary (fig. 9*b* and *c*).

In the acariform mite *Archegozetes longisetosus*, the single-copy homologs of *dac* and *exd* were expressed comparably to their *P. opilio* counterparts. A ring of *Al-exd* expression in juxtaposition with, and distal to, the *Al-dac* domain was observed in the palp and legs of the hexapodous larva at the limb bud stage (fig. 9*d*).

In the appendages of the solifuge *Titanopuga salinarum*, expression of the single-copy *Ts-exd* and *Ts-dac* homologs was largely consistent with expression patterns observed in other surveyed taxa (fig. 9*e*–*h*). The chelicerae exhibit strong expression of *Ts-exd* in both podomeres (fig. 9*e*, 9*e*′). A domain of *Ts-dac* was detected in the proximal territory of the chelicera, as has previously been described for the mite *A. longisetosus* (Barnett and Thomas 2013). In the pedipalps and first two pairs of walking legs, *Ts-dac* was expressed in the presumptive trochanter and femur, whereas *Ts-exd* was expressed in both a proximal territory encompassing the coxa and trochanter, and a distal ring domain adjacent to the medial *Ts-dac* expression (fig. 9*f*–*h*). This distal expression suggests that the "post-femur" of some authors can be homologized to the patella

Downloaded from https://academic.oup.com/mbe/article/41/9/msae188/7749772 by guest on 11 October 2024

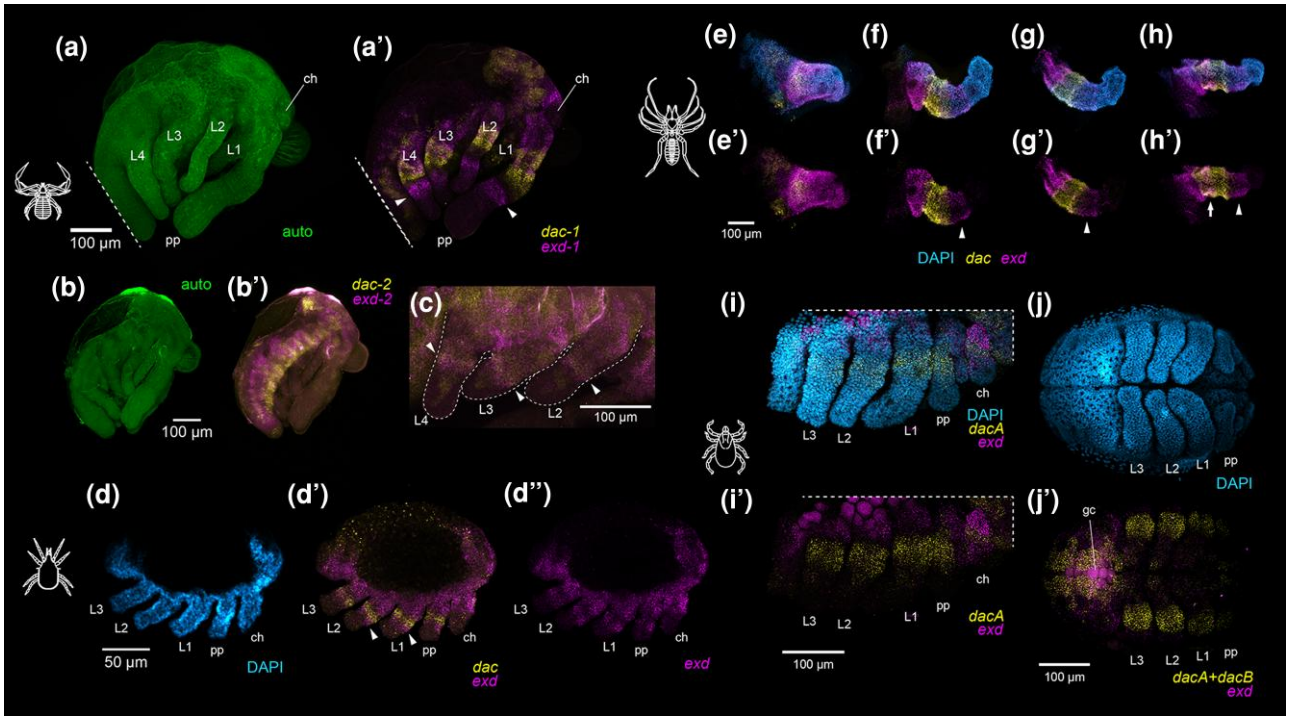

Fig. 9. Surveys of *exd* and *dac* expression across arachnid orders with disputed patellar homologs. (**a**) Embryo of the pseudoscorpion *Pselaphochernes scorpioides* visualized via cuticular autofluorescence (green). (**a**′) Same embryo as in (**a**) with multiplexed expression of *Ps-exd-1* (magenta) and *Ps-dac-1* (yellow). (**b**) Autofluorescent visualization of *P. scorpioides* embryo. (**b**′) Same embryo as in (**b**) with expression of *Ps-exd-2* and *Ps-dac-2*. (**c**) Magnified view of *Ps-exd-2* and *Ps-dac-2* expression in the legs of an older *P. scorpioides* embryo. (**d**) Limb bud stage embryo of the acariform mite *Archegozetes longisetosus* with Hoechst nuclear counterstaining (cyan). (**d**′, **d**″) Same embryo as in (**d**) with multiplexed expression of *Al-exd* (magenta) and *Al-dac* (yellow) (**d**′), or single-channel expression of *Al-exd* (**d**″). (**e**–**h**) Limb mounts of the solifuge *Titanopuga salinarum* at leg elongation stage with nuclear counterstaining (cyan), and expression of *Ts-exd* (magenta) and *Ts-dac* (yellow). (**e**, **e**′) Chelicera. (**f**, **f**′) Pedipalp. (**g**, **g**) Leg one. (**h**, **h**′) Leg three. Note additional domain of overlapping *dac* and *exd* in the basifemur of leg three (unique to legs three and four; white arrow). White arrowheads indicate an *exd* boundary distal of *dac*. Abbreviations: ch, chelicera; pp, pedipalp; L1, leg one; L2, leg two; L3, leg three; L4, leg four. (**i**) Stage 9 embryo of the tick *Ixodes scapularis* with Hoechst nuclear counterstaining (cyan), *Is-dacA* expression (yellow), and *Is-exd* expression (magenta). (**e**′) Same embryo as in (**e**) without nuclear counterstaining. (**j**) Stage 10 embryo of *I. scapularis* with nuclear counterstaining. (**j**′) Same embryo as in (**j**) showing multiplexed expression of *Is-dacA* and *Is-dacB* (yellow), and *Is-exd* (magenta). Note autofluorescence of yolk and germ cells (gc) in magenta channel in (**i**′, **j**′).

(Millot 1949; Punzo 1998), consistent with the nomenclature of Shultz (1989). The third and fourth walking legs also exhibited the conserved proximal and distal domains of *Ts-exd*, and medial domain of *Ts-dac* (fig. 9*h*, 9*h*′). In contrast to the pedipalp or the first two leg pairs, an additional domain comprised of overlapping *Ts-dac* and *Ts-exd* expression was observed in the additional segment, the presumptive basifemur (sensu Shultz 1989). Presence of the non-overlapping distal *Ts-exd* domain again supports retention of a patellar homolog and refutes previous interpretations of a subdivided trochanter and a subdivided femur condition in the third and fourth solifuge leg (Millot 1949; Punzo 1998).

In the genome assembly of the tick *Ixodes scapularis*, we discovered two copies of *dac* and one copy of *exd*. Gene tree analysis of the tick *dac* paralogs suggested independent origins with respect to the arachnopulmonate copies. When multiplexed in a single channel, the two *dac* copies (*Is-dacA*, *Is-dacB*) exhibited comparable dynamics with respect to the single-copy harvestman homolog, spanning the trochanter, basifemur, and distifemur (fig. 9*j*). Segmental identities were extrapolated from the extent of *Is-dac* expression in stage 24 embryos wherein podomere boundaries are clearly visible (supplementary fig. S9, Supplementary Material online). Surprisingly, *Is-exd* expression was detected only in the body wall, coxa, and trochanter; we did not detect *Is-exd* expression as a ring distal to the *Is-dac* paralogs in any stages surveyed (fig. 9*i* and *j*).

Discussion

A Phylogenetically Consistent Mechanism for Patellar Origin

Developing mechanistic connections between genotype and phenotype is a fundamental goal of evolutionary developmental biology. Crucially, in comparative development contexts, the putative genetic mechanism underlying a novel trait must be compatible with the phylogenetic distribution of that trait. Here, we investigated the fit of a putative developmental mechanism for patellar origin using a phylogenetic test and showed that the phylogenetic distribution of *dac-2*, which is restricted to Arachnopulmonata, is inconsistent with the interpretation that the origin of this gene copy underlies the patterning of the patellar segment

Downloaded from https://academic.oup.com/mbe/article/41/9/msae188/7749772 by guest on 11 October 2024

across Chelicerata. Paralleling this case, expression surveys of other paralogous genes in spider models have prompted inferences of neofunctionalization that exhibit similar mismatch of phylogenetic distribution between gene and trait. In one case, expression of *hth-1* reflects patterns found in arthropods broadly, whereas *hth-2* is expressed as a series of distal ring domains that vary across spider lineages (Turetzek et al. 2017). The authors took these expression differences to mean neofunctionalization of the duplicated *hth-2* copy, in addition to the inference that changes in the number of *hth-2* expression rings across spiders were mechanistically meaningful with regard to differences in appendage morphology across spider taxa. However, it was later shown that a similar division of expression domains is observed across both copies of *hth* in scorpions and whip spiders, while broader taxonomic sampling of *hth* has subsequently implicated its origin as a result of the arachnopulmonate whole genome duplication. (Sharma et al. 2012a; Gainett and Sharma 2020; Nolan et al. 2020). Thus, while the functional significance of their expression dynamics remain unknown, the incidence of the *hth-2* paralog is demonstrably not spider-specific, nor do the expression levels of *hth-2* paralogs correlate with specific leg phenotypes (Sharma 2023). As a second example, expression of one paralog of the paired box gene *Pax2* in the lateral eyes of spiders was taken to suggest subfunctionalization of ancestral pleiotropic functions in brain, appendage, and eye development, as well as a key role in differentiating the lateral eyes from the median eyes (Janeschik et al. 2022). However, a recent work refuted a role for *Pax2* as an eye marker specific to lateral eyes; the single copy homolog of *Pax2* is expressed in both the median eyes and vestigial lateral eyes of harvestmen, whereas both orthologs of *Pax2* in the scorpion are also expressed in median and lateral eye primordia (Gainett et al. 2024a). These patterns suggest that the dynamics of *Pax2-1* in the developing eyes of spiders are a taxon-specific phenomenon and do not reflect the ancestral condition of *Pax2* homologs across Chelicerata.

These previous interpretations of neofunctionalization based on spider expression patterns have substantiated the perception that the morphological evolution of chelicerates has been largely shaped by whole genome duplication and neofunctionalization of paralogs, despite a dearth of functional studies that link new genes to new phenotypes in arachnopulmonates (Sharma 2023). Our work suggests instead that novel traits can be established by the rewiring of existing gene regulatory networks comprised of ancient genes (e.g. Davidson and Erwin 2006; Anderson et al. 2016; Höch et al. 2021; Babonis et al. 2023). In support of this interpretation, we have demonstrated that the acquisition of a novel expression domain by the conserved appendage patterning gene *extradenticle* is essential for establishment of the patellar segment. While divergence of paralog expression domains across arachnopulmonates is a compelling phenomenon, understanding their role in the evolution of novel traits requires functional studies to substantiate hypotheses of neofunctionalization. As shown here in the case of *dac-2*, functional data must also be paired with broader taxonomic sampling and comparative gene expression, toward applying a phylogenetic test of putative genotype-phenotype connections. More generally, surveys outside the focal study taxon are essential to polarizing developmental phenomena. The increasing availability of genomic resources and functional techniques for diverse model species spanning animal diversity, as demonstrated herein through the first gene expression surveys for multiple chelicerate orders, foretells a more robust framework for future investigations of comparative developmental mechanisms.

The Developmental Dynamics of Arachnopulmonate *dachshund* are Consistent With Subfunctionalization

The coincidence of the phenotype incurred by knockdown of *Po-exd* and *dac-2* in the spider *P. tepidariorum* is remarkable and invited our reinvestigation of *dac* in chelicerate appendage evolution. This coincident loss-of-function phenotype could be interpreted as a case of developmental system drift, wherein the divergence of genetic mechanisms across taxa does not affect a trait's expression. Alternatively, the function of *dac-2* in spiders may reflect the subdivision of an older role for *dac* in establishing the segmental boundaries of medial leg segments. Apropos, *dac* loss-of-function phenotypes in other arthropod models have suggested a role for *dac* in appendage segmentation. As examples, loss-of-function *dac* mutants in *D. melanogaster* exhibit a fusion of the a5-arista joint in the antenna, whereas *dac* is known to be required for establishing the segment-forming domains of *Notch* and *fringe* in the walking leg (Dong et al. 2001). Similarly, weak knockdown of *dac* results in fusion of the femur-tibia joint in the hemipteran *Oncopeltus fasciatus* (Angelini and Kaufman 2004), and larval RNAi against *dac* in the beetle *Tribolium castaneum* incurs fusions of the first three tarsal articles (Angelini et al. 2012). These phenotypes are consistent with the observation that *dac* null mutants exhibit increased cell death in the presumptive medial territory of leg imaginal discs of *D. melanogaster* (Mardon et al. 1994).

The loss of segment boundaries in late *Po-dac* RNAi embryos is consistent with phenotypic spectra of *dac* homologs across the arthropod tree of life and suggests conserved roles for *dac* in the growth of the medial territory and regulation of segmentation in the medial segments. With respect to spider *dac-2*, our results suggest that the previously described function of the spider *dac* duplicate copy does not reflect neofunctionalization (Turetzek et al. 2016), as much as a subdivision of the ancestral function between the two arachnopulmonate-specific daughter copies. Consistent with this interpretation, the phenotypic spectrum of *Po-dac* encompasses the phenotype exhibited by spider *dac-2* RNAi hatchlings (patella-tibia fusions). In addition, the irregular outgrowth at the fused patella-tibia boundary in *P. tepidariorum dac-2* RNAi hatchlings resemble morphogenetic defects described in insect *dac* RNAi experiments (Angelini and Kaufman 2004).

Downloaded from https://academic.oup.com/mbe/article/41/9/msae188/7749772 by guest on 11 October 2024

As a test of our interpretation, future experiments should reexamine *exd-1* and *exd-2* loss-of-function phenotypes in the spider to assess whether RNAi against one or both *exd* copies recapitulates the RNAi phenotype obtained in the harvestman. Functional data for spider *dac-1* are also sorely needed to validate interpretation of either sub- or neofunctionalization. However, we add the caveat that inherent limits on the effectiveness of RNAi in *P. tepidariorum* may hinder functional investigations of leg patterning in that species. As an example, we trialed maternal RNAi against *exd-1* and *exd-2* in this study, following previous approaches to RNAi in *P. tepidariorum* (Akiyama-Oda and Oda 2006; Khadjeh et al. 2012; Setton and Sharma 2018). We observed no morphological defects in those experiments, with all embryos and hatchlings exhibiting wild type morphology (data not shown). Similarly, our efforts to evince the role of *dac-1* in several aspects of spider morphogenesis (e.g. leg patterning; neurogenesis; eye development) have repeatedly met with the same result in *P. tepidariorum* (data not shown).

A Patella was Present in the Common Ancestor of Chelicerata

Together with existing expression data in spider and scorpion models (Prpic et al. 2003; Nolan et al. 2020), the demonstration of a distal *exd* domain in harvestmen, acariform mites, solifuges, and pseudoscorpions underscores widespread conservation of patellar homologs across terrestrial arachnids. Retention of the distal ring in Pycnogonida likewise supports the presence of the patella in the common ancestor of Chelicerata (fig. 10), as previously advocated in some of the early morphological works (Snodgrass 1958; Dencker 1974; Schram and Hedgpeth 1978; Shultz 1989; Sabroux et al. 2023). As such, it seems that historical confusion and terminological mismatches in the arthropod literature may largely reflect an overreliance on morphometrics and perceived differences in podomere function, rather than strict interpretations of homology (reviewed in Shultz [1989]). Instead, broad congruence in both the number of appendage podomeres and patterns of muscle insertion sites across chelicerate orders supports a more unified nomenclature, with recognition of taxon-specific gains, subdivisions, or loss of podomeres (Shultz 1989).

The clear functional link between the distal ring domain of *exd* expression and establishment of the patellar segmental boundary highlights the utility of evolutionary developmental biology in resolving long-standing and often contentious interpretations of homology in anatomical structures. As other examples within Arthropoda, the function of retinal determination genes in harvestmen revealed vestiges of the lateral eyes and an additional pair of median eyes, whereas external morphology had long suggested retention of only a single pair of median eyes in this group (Gainett et al. 2024a). Similarly, surveys of Hox gene expression have advanced the understanding of the "arthropod head problem", a question of positional homology of head structures in this phylum. Such surveys famously established the homology of sea spider chelifores, arachnid chelicerae, and mandibulate (first) antennae as deutocerebral structures (Jager et al. 2006).

Despite improved resolution of patellar homology and evolutionary origin, the trait cannot be universally applied to all chelicerate taxa. The absence of distal *exd* expression in the parasitiform tick *I. scapularis* impels two alternative interpretations. First, it is possible that ixodid ticks have lost a patellar homolog, justifying the previous use of genu for the fifth podomere identity. Alternatively, Ixodida may have acquired either a novel genetic mechanism for patellar patterning or repurposed an existing appendage patterning gene to this end, exemplifying developmental system drift. The presence of two *dac* copies in the *I. scapularis* genome is particularly intriguing in this regard and invites interrogation of divergent paralog function following tandem duplication. The recent advent of gene editing tools in *I. scapularis* offers a promising vehicle for functional investigation of *dac* function in this system (Sharma et al. 2022). Notably, two other chelicerate orders have occasionally been suggested to lack patellar homologs. The pedipalps and walking legs of Palpigradi (microwhip scorpions) are thought to possess a genu in the identical PD axis position of the patella in other groups (van der Hammen 1982), whereas Ricinulei (hooded tick spider) pedipalps place the femur in that position, by nature of possessing two trochanters (Pittard and Mitchell 1972). The small size, difficulty of collection, and dearth of functional resources for these organisms presently prevents analysis of segmental homologies. Yet, recent phylogenetic affinities of these groups may yield more parsimonious hypotheses. The most comprehensive analysis of higher-level chelicerate relationships consistently recovered a sister group relationship of palpigrades and the clade containing both Acariformes and Solifugae with support (Ballesteros et al. 2022). As such, it is likely that palpigrades retain a patellar homolog, rather than genu, given its presence in both sister taxa. But in the same analyses, Ricinulei are recovered as sister group to Parasitiformes, and without resolution of segmental affinity in *I. scapularis*, suggests that Ricinulei may also lack a patellar homolog.

Beyond the homology of the patella, chelicerate podomeres remain rife with unresolved homology disputes and questionable ancestral states (supplementary tables S1 and S2, Supplementary Material online). The most prominent example is the condition of the femur, which is retained as a single podomere in most extant lineages (Arachnopulmonata, Opiliones, Palpigradi, Xiphosura), but is subdivided into basifemur and telofemur in groups such as Parasitiformes and Acariformes. Likewise, presence of an additional podomere in walking legs III and IV in Solifugae and Ricinulei is often described as either an additional trochanter or femur; the identification of a novel overlapping domain of *dac* and *exd* in legs III and IV of a solifuge embryo in this study (compare fig. 9*g* and *h*) provide the first clues of how this additional podomere may be patterned. Reconstruction of the ancestral condition is further

Downloaded from https://academic.oup.com/mbe/article/41/9/msae188/7749772 by guest on 11 October 2024

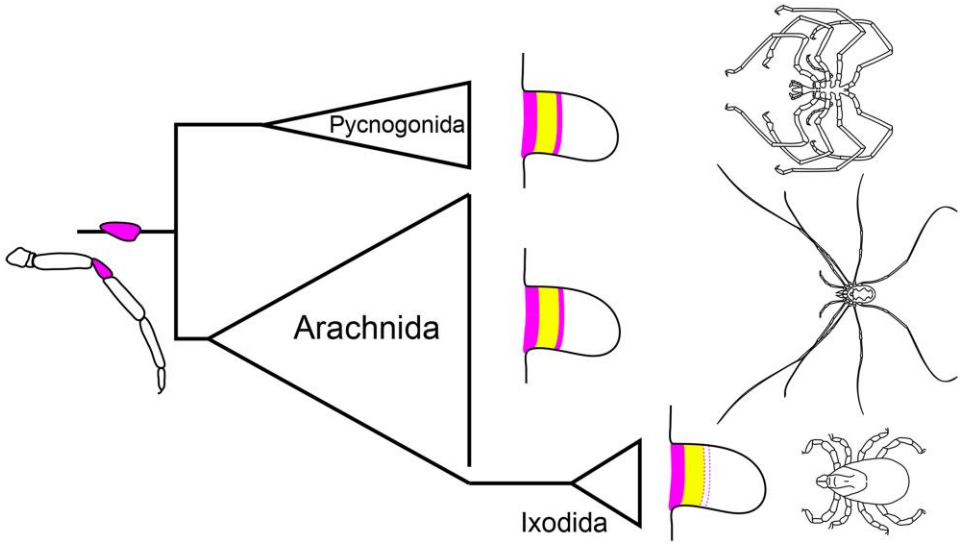

Fig. 10. A distal ring domain of exd, abutting a conserved medial domain of *dac*, during embryonic appendage formation is responsible for the origin of the chelicerate patella. Presence of the distal ring domain in Pycnogonida and many chelicerate orders supports its presence in the chelicerate common ancestor. Lineage-specific loss of distal *exd* expression in ixodid ticks suggests loss of a patellar homolog.

confounded by the additional proximal segmentation in Pycnogonida, with many taxonomists inferring the presence of three coxae and a single femur. This scheme therefore suggests an undivided femur as the likely ancestral chelicerate condition. Here, we have demonstrated strong expression of *exd* in the distal compartment of the still undivided femur-tibia 1 precursor podomere of the *P. litorale* instar IV, homologizing the proximal tibia 1 of sea spiders with the patella. This placement of the patella as the fifth podomere along the PD axis is reminiscent of the placement of the patella in Solifugae or non-oribatid Acariformes, groups possessing a subdivision of the femur. Application of this podomere terminology therefore aligns the three coxae and single femur of pycnogonids with coxa, trochanter, basifemur, and telofemur, potentially supporting the subdivision of femora as the ancestral state in Chelicerata. Descriptions of fossilized chelicerate lineages reinforce this interpretation. Unlike extant horseshoe crabs that possess five post-coxal segments, extinct synziphosurines, such as *Offacolus* and *Dibasterium*, retain six post-coxal segments (Sutton et al. 2002; Briggs et al. 2012). Many eurypterid taxa also possess additional segments in their third and fourth walking legs, represented as either a bipartite femur or trochanter (Selden 1981). Recent total evidence analysis placing Eurypterida and synziphosurines as part of a clade within the larger Merostomata (Ballesteros et al. 2022) further suggests secondary fusion of proximal segments in extant horseshoe crabs.

Patterns of muscle attachments also lend credence to the inference that the ancestral femur was subdivided (see Shultz [1989]). In *Limulus* (Xiphosura), Araneae, and Amblypygi, two muscles arise in the anterior trochanter, span the trochanter-femur joint diagonally, and insert in the proximoposterior femur. Yet, these muscles lack tendon insertions, obscuring their function. Both have been homologized with the depressor muscle spanning the basifemur-telofemur joint of Solifugae. Likewise, Amblypygi and Schizomida both possess a muscle arising in the anterior of the trochanter that inserts distally into the dorsal midline of the femur, without means of a tendon. This muscle has been homologized with the basifemur-telofemur levator in Solifugae. These unusual patterns are suggestive of a former mobile joint that has secondarily fused in groups like extant tetrapulmonates. Certain members of the extinct Trigonotarbida (putatively sister to Tetrapulmonata; Ballesteros et al. 2022) and extinct lineages of Araneae, Amblypygi, and Uropygi also possess appendages that have been reconstructed with an additional podomere between trochanter and femur (Shear et al. 1987).

Given the comparative framework, new study systems, and genomic resources established in this study, future investigations are well poised to address the ancestral condition of proximal segmentation in Chelicerata. Such investigations should prioritize identification of transcription factors that establish basi- and telofemoral identities in model taxa, with the goal of surveying the same mechanisms in groups like Pycnogonida, Solifugae, and Acariformes to polarize podomere evolution across the chelicerate tree of life.

Materials and Methods

RNA Sequencing

Brooding females and nymphal stages of the pseudoscorpion *Pselaphochernes scorpioides* were collected from compost bins in Madison, Wisconsin (43°04′43.8″N, 89°23′12.1″W) in July 2022 and June 2023 (voucher specimens lodged in Western Australian Museum). A subset of eggs and juveniles were fixed in TRIzol TriReagent (Thermofisher) for RNA extraction. For the solifuge *Titanopuga salinarum*, three juveniles were collected in Córdoba, Argentina (64°48′S, 30°02′W) in December 2023 and brain tissue was dissected in phosphate buffered saline (PBS) and fixed in RNA*later*, with subsequent transfer to TRIzol. Total RNA was extracted from these samples and purified mRNA was sequenced on an Illumina NovaSeq platform at the UW-Madison BioTechnology Center, following our previous strategy for library preparation (Ontano et al. 2021). Transcriptomic assembly was

Downloaded from https://academic.oup.com/mbe/article/41/9/msae188/7749772 by guest on 11 October 2024

performed using Trinity v. 2.15 (Grabherr et al. 2011); for the solifuge, the reads obtained in this study were combined with previous developmental transcriptomes to generate a new assembly (Gainett et al. 2024b). A developmental transcriptome of the sea spider *P. litorale* was previously generated from pooled embryos and postembryonic instars reared in a laboratory culture at Greifswald University, Germany (Brenneis et al. 2023). All developmental stages were fixed and stored in RNAlater for RNA extraction.

Bioinformatics and Phylogenetic Analysis

Homologs of *extradenticle*, *dachshund*, *Notch*, and *engrailed* were identified in the genome of *Phalangium opilio* (Gainett et al. 2021) and sequence identities confirmed by alignment against transcripts from previous studies in this species (Sharma et al. 2012a, 2012b), as well as using SMART-BLAST. Homologs of *extradenticle* and *dachshund* were additionally extracted from the transcriptomes of the sea spider *Pycnogonum litorale* (Brenneis et al. 2023), the pseudoscorpion *P. scorpioides* (this study), and the solifuge *Titanopuga salinarum* (Gainett et al. 2024b; this study); and from the genomes of the mite *Archegozetes longisetosus* (Brückner et al. 2022) and the tick *Ixodes scapularis* (Nuss et al. 2023). For *dac* and *exd*, peptide translations of nucleotide sequences were added to a previous alignment of panarthropod homologs (Nolan et al. 2020; Ontano et al. 2021) and multiple sequence alignment was performed de novo with CLUSTAL Omega (Sievers and Higgins 2018). Gene trees were inferred using IQ-TREE v. 1.6.12 (Nguyen et al. 2015) with an LG + I + G substitution model and nodal support was estimated using 1,000 ultrafast bootstrap replicates. Alignments are provided in supplementary files S1 and S2, Supplementary Material online. Gene trees are provided in supplementary files S3 and S4, Supplementary Material online.

Embryo Collection, Fixation, and In Situ Hybridization

Embryos were fixed and assayed for fluorescent detection of gene expression following established or minimally modified protocols, as detailed previously for *P. opilio* (Gainett et al. 2021) and *A. longisetosus* (Barnett and Thomas 2013). Adult females of *T. salinarum* were collected from the same locality as the juveniles used in RNA sequencing. Females were housed and resulting embryos fixed and assayed as in Gainett et al. (2024b).

For *P. scorpioides*, embryos were dissected out of the broodsac with fine forceps and transferred to 2 mL Eppendorf tubes. Embryos were fixed in a solution of 3.2% paraformaldehyde in 1× PBS for 20 min, followed by washes in 1× PBST (0.1% Tween-20) and gradual dehydration into 100% methanol.

For *I. scapularis*, pathogen-free, unfed adults were acquired from Oklahoma State University Centralized Tick Rearing Facility and were maintained in an environmental chamber at 20 °C and 95% relative humidity (RH) at the University of Nevada-Reno. Adult ticks were fed on New Zealand White rabbits (Reyes et al. 2020) until fully engorged. Gravid females were collected and placed into individual transparent containers for egg-laying at 20 °C and 95% RH. Oviposition began 6 to 14 d after collection and eggs were harvested daily into 1.5 mL microcentrifuge tubes. To fix, eggs were transferred to a 70 µm cell strainer (EASYstrainer, Greiner Bio-One) and washed for 3 min in 8% sodium hypochlorite while agitating with a paintbrush. Eggs were subsequently washed three times with deionized (DI) water. Using a paintbrush, the eggs were then transferred into PCR tubes with 100 µL of DI water and incubated at 90 °C for 3 min followed by snap cooling at −20 °C for an additional 3 min before thawing at ambient temperature. DI water was then removed and replaced with a 1:1 ratio of 4% paraformaldehyde and heptane. Eggs were allowed to fix at ambient temperature on a vortex mixer for 1 h or overnight. The paraformaldehyde layer was removed and replaced with an equal volume of 100% methanol and tubes were vigorously shaken for 1 to 2 min. Following fixation, embryos were stored at 4 C until ready for use. All procedures involving animal subjects were approved by the Institutional Animal Care and Use Committee (IACUC) at the University of Nevada-Reno (IACUC #21-01-1118-1).

For *P. litorale*, postembryonic instars were reared in the in-house laboratory culture at the Animal Facility at University of Vienna. Instars II to IV were collected from their host, the hydrozoan *Clava multicornis*. After relaxation for 1 to 2 min in freshly carbonated artificial seawater (ASW; 32‰), specimens were fixed in 4% paraformaldehyde in ASW for 1 h at ambient temperature, washed two times in ASW, gradually transferred into 1× PBS, followed by gradual dehydration into 100% methanol. Samples were stored at −20 °C until further use. Prior to HCR-FISH, the instars were gradually rehydrated into 1× PBS and exposed to 5 to 10 brief pulses in a bath ultrasonicator to enhance cuticle permeability.

Probe design for hybridization chain reaction (HCR) consisted of 12 to 30 probe pairs, depending upon the length of the available template sequence. Probes were designed either with the HCR Probe Maker tool (Kuehn et al. 2022), or via submission of CDS to Molecular Instruments. Input CDS templates for proprietary Molecular Instrument probe design and probe sequences obtained from the HCR Probe Maker tool for all six chelicerate species are provided in supplementary file S5, Supplementary Material online (supplementary tables S3 to S19, Supplementary Material online).

Cloning of Orthologs, dsRNA Synthesis, and RNAi

Fragments of *Po-exd* and *Po-N* were amplified using standard PCR protocols and cloned using a TOPO TA Cloning Kit using One Shot Top10 chemically competent *Escherichia coli* (ThermoFisher) following the manufacturer's protocol, and their PCR product identities were verified via Sanger sequencing with M13 universal primers. A plasmid containing a sequence of *Po-dac* was available from a previous study (Sharma et al. 2013). All gene-specific primer sequences are provided in supplementary file S5,

Downloaded from https://academic.oup.com/mbe/article/41/9/msae188/7749772 by guest on 11 October 2024

Supplementary Material online (supplementary table S20, Supplementary Material online). Double-stranded RNA (dsRNA) was synthesized following the manufacturer's protocol using a MEGAscript T7 kit (Ambion/Life Technologies) from amplified PCR product. The quality of dsRNA was assessed and concentrations adjusted using a NanoDrop ONE to 3.7 to 4 µg/µL. dsRNA was mixed with vital dyes for visualization of injections. Microinjection under halocarbon-700 oil (Sigma-Aldrich) was performed as previously described (Sharma et al. 2013). Subsets of developing embryos were fixed for HCR and assayed for selected genes.

Scoring of phenotypes divided embryos into three discrete categories. Embryos scored as dead exhibited early developmental arrest and/or visible decomposition; these were inferred to result from a combination of dsRNA toxicity, microinjection error, and associated off-target effects. Embryos scored as phenotypes exhibited morphological defects after at least 72 h post-injection. Embryos scored as wildtype exhibited no overt morphological defects, consistent with wildtype morphogenesis. For *Po-dac* and *Po-exd* late RNAi experiments, embryos were raised until hatching; in cases of severe defects, embryos were manually dissected from the vitelline membrane to assist hatching. For *Po-N* RNAi experiments, embryos were fixed between 72 and 96 h post-injection, given the degree of defects incurred by knockdown of *Notch*.

Imaging

Brightfield microscopy was performed using a Nikon SMZ fluorescence stereomicroscope mounted with a DSFi2 digital color camera and driven by Nikon Elements software. SEM was performed using a Quanta FEI 200 scanning electron microscope. Confocal laser scanning microscopy was performed using a Zeiss LSM 780 microscope driven by Zen software. For *P. litorale*, confocal laser scanning microscopy was performed with a Leica SP5 microscope, driven by LAS-AF software. Beyond the documentation of gene expression (594 and 633 nm laser lines) and DAPI counterstain (405 nm laser line), cuticular autofluorescence was separately recorded with the 488 nm laser line. Using the software Amira 3D (version 2021.1; ThermoFisher Scientific), the cuticular signal in the 488 nm channel was semi-automatically segmented (grey-value based thresholding) and the voxels included in the resulting material were set to grey value 0 in all other channels via the "Arithmetic" function, resulting in the separation of cuticular autofluorescence from gene expression signals.

Supplementary Material

Supplementary material is available at *Molecular Biology and Evolution* online.

Acknowledgments

Microscopy was performed at the Newcomb Imaging Center, Department of Botany, University of Wisconsin-Madison, with the aid of Sarah Swanson. The LABRE team and Gabriel Boaglio provided support during collecting trips in Argentina. Diego M. Fink assisted with shipment of solifuge embryos. Hugh G. Steiner and Pola O. Blaszczyk assisted with maintenance of *P. opilio*. Hypatia Coop in Madison (WI) kindly assisted with collection of pseudoscorpion embryos. Marion Wanninger and Max Hämmerle assisted with the maintenance of *P. litorale*. G.B. thanks Andreas Wanninger for providing research infrastructure. Discussions with Armin Moczek refined some of the experiments addressing *dac* subfunctionalization. Comments from two anonymous reviewers refined ideas presented in the manuscript. This work was funded by the National Science Foundation grant no. IOS-2016141 to P.P.S; and National Institutes of Health NIAID grant nos. R21AI128393, R212200536 and R012200185 to M.G.-N.

Author Contributions

B.C.K. and P.P.S. designed the objectives of the study. B.C.K., E.M.L., S.M.N., G.M.H., G.G., E.V.W.S., and P.P.S. performed functional experiments. B.C.K., E.M.L., S.M.N., G.G., and P.P.S. generated data for *P. opilio*. N.H.P. contributed tools and reagents for analyses, and sponsored the Whitman Fellowship for P.P.S. for arachnid tool development. G.B. generated data for *P. litorale*. A.A.B. and I.J. generated data for *A. longisetosus*. B.C.K. and I.A.H. generated data for *I. scapularis*. B.C.K., C.S., and D.E.V. field collected females and fixed resulting embryos of *T. salinarum*. B.C.K., G.G., E.V.W.S., and P.P.S. collected embryos and females of *P. scorpioides*. B.C.K. and P.P.S. performed RNA extraction and transcriptome assembly. B.C.K. generated expression data for *T. salinarum* and *P. scorpioides*. B.C.K., G.G., E.V.W.S., I.A.H., A.A.B., and G.B. performed bioinformatics. B.C.K., G.B., and P.P.S. wrote the first draft of the manuscript. B.C.K., M.S.H., G.B., and P.P.S. created figures and tables. P.P.S. and M.G.-N. procured funding.

Data Availability

All image data are published in the manuscript or as supplementary material. All genomic resources are publicly available on NCBI.

References

Akiyama-Oda Y, Oda H. Axis specification in the spider embryo: *dpp* is required for radial-to-axial symmetry transformation and *sog* for ventral patterning. Development. 2006:**133**(12):2347–2357. https://doi.org/10.1242/dev.02400.

Anderson DP, Whitney DS, Hanson-Smith V, Woznica A, Campodonico-Burnett W, Volkman BF, King N, Thorton JW, Prehoda KE. Evolution of an ancient protein function involved in organized multicellularity in animals. eLife. 2016:**5**:e10147. https://doi.org/10.7554/eLife.10147.

Angelini DR, Kaufman TC. Functional analyses in the hemipteran *Oncopeltus fasciatus* reveal conserved and derived aspects of appendage patterning in insects. Dev Biol. 2004:**271**(2):306–321. https://doi.org/10.1016/j.ydbio.2004.04.005.

Angelini DR, Kaufman TC. Comparative developmental genetics and the evolution of arthropod body plans. Annu Rev Genet.

Downloaded from https://academic.oup.com/mbe/article/41/9/msae188/7749772 by guest on 11 October 2024

2005:**39**(1):95–119. https://doi.org/10.1146/annurev.genet.39.073003.112310.
Angelini DR, Kikuchi M, Jockusch EL. Genetic patterning in the adult capitate antenna of the beetle *Tribolium castaneum*. Dev Biol. 2009:**327**(1):240–251. https://doi.org/10.1016/j.ydbio.2008.10.047.
Angelini DR, Smith FW, Jockusch EL. Extent with modification: leg patterning in the beetle *Tribolium castaneum* and the evolution of serial homologs. G3. 2012:**2**(2):235–248. https://doi.org/10.1534/g3.111.001537.
Arnaud F, Bamber RN. The biology of pycnogonida. In: Blaxter JHS, Southward AJ, editors. Advances in marine biology. Vol. 24. London, UK: Academic Press; 1988. p. 1–96.
Babonis LS, Enjolras C, Reft AJ, Foster BM, Hugosson F, Ryan JF, Daly M, Martindale MQ. Single-cell atavism reveals an ancient mechanism of cell type diversification in a sea anemone. Nat Commun. 2023:**14**(1):885. https://doi.org/10.1038/s41467-023-36615-9.
Ballesteros JA, Santibáñez-López CE, Baker CM, Benavides LR, Cunha TJ, Gainett G, Ontano AZ, Setton EVW, Arango CP, Gavish-Regev E, et al. Comprehensive species sampling and sophisticated algorithmic approaches refute the monophyly of Arachnida. Mol Biol Evol. 2022:**39**(2):msac021. https://doi.org/10.1093/molbev/msac021.
Ballesteros JA, Santibáñez López CE, Kováč Ľ, Gavish-Regev E, Sharma PP. Ordered phylogenomic subsampling enables diagnosis of systematic errors in the placement of the enigmatic arachnid order Palpigradi. Proc Biol Sci. 2019:**286**(1917):20192426. https://doi.org/10.1098/rspb.2019.2426.
Ballesteros JA, Sharma PP. A critical appraisal of the placement of Xiphosura (Chelicerata) with account of known sources of phylogenetic error. Syst Biol. 2019:**68**(6):896–917. https://doi.org/10.1093/sysbio/syz011.
Barnett AA, Thomas RH. The expression of limb gap genes in the mite *Archegozetes longisetosus* reveals differential patterning mechanisms in chelicerates. Evol Dev. 2013:**15**(4):280–292. https://doi.org/10.1111/ede.12038.
Brenneis G, Bogomolova EV, Arango CP, Krapp F. From egg to "nobody": an overview and revision of developmental pathways in the ancient arthropod lineage Pycnogonida. Front Zool. 2017:**14**(1):6. https://doi.org/10.1186/s12983-017-0192-2.
Brenneis G, Frankowski K, Maaß L, Scholtz G. The sea spider *Pycnogonum litorale* overturns the paradigm of the absence of axial regeneration in molting animals. Proc Natl Acad Sci U S A. 2023:**120**(5):e2217272120. https://doi.org/10.1073/pnas.2217272120.
Briggs DEG, Siveter Derek J, Siveter David J, Sutton MD, Garwood RJ, Legg D. Silurian horseshoe crab illuminates the evolution of arthropod limbs. Proc Natl Acad Sci U S A. 2012:**109**(39):15702–-15705. https://doi.org/10.1073/pnas.1205875109.
Bruce HS, Patel NH. Knockout of crustacean leg patterning genes suggests that insect wings and body walls evolved from ancient leg segments. Nat Ecol Evol. 2020:**4**(12):1703–1712. https://doi.org/10.1038/s41559-020-01349-0.
Brückner A, Barnett AA, Bhat P, Antoshechkin IA, Kitchen SA. Molecular evolutionary trends and biosynthesis pathways in the oribatida revealed by the genome of *Archegozetes longisetosus*. Acarologia. 2022:**62**(2):532–573. https://doi.org/10.24349/pjye-gkeo.
Brunet FG, Crollius HR, Paris M, Aury J-M, Gibert P, Jaillon O, Laudet V, Robinson-Rechavi M. Gene loss and evolutionary rates following whole-genome duplication in teleost fishes. Mol Biol Evol. 2006:**23**(9):1808–1816. https://doi.org/10.1093/molbev/msl049.
Brusca RC, Brusca GJ. Invertebrates. 2nd ed. Sunderland (MA): Sinauer Associates; 2003.
Cai J, Zhao R, Jiang H, Wang W. De novo origination of a new protein-coding gene in *Saccharomyces cerevisiae*. Genetics. 2008:**179**(1):487–496. https://doi.org/10.1534/genetics.107.084491.
Carpio R, Honoré SM, Araya C, Mayor R. *Xenopus paraxis* homologue shows novel domains of expression. Dev Dyn. 2004:**231**(3):609–613. https://doi.org/10.1002/dvdy.20147.
Chen Y, Li H, Yi T-C, Shen J, Zhang J. Notch signaling in insect development: a simple pathway with diverse functions. Int J Mol Sci. 2023:**24**(18):14028. https://doi.org/10.3390/ijms241814028.
Davidson EH, Erwin DH. Gene regulatory networks and the evolution of animal body plans. Science. 2006:**311**(5762):796–800. https://doi.org/10.1126/science.1113832.
de Beer GR. Embryology and evolution. Hum Mente. 1930:**5**:482–484.
Dencker D. Das Skeletmuskelsystem von *Nymphon rubrum* Hodge, 1862 (Pycnogonida: Nymphonidae). Zool Jahrb Abt Anat Ontog Tiere. 1974:**93**:272–287.
Dittmar K, Liberles D. Evolution after gene duplication. Hoboken (NJ): John Wiley & Sons, Inc.; 2011.
Dong PDS, Chu J, Panganiban G. Proximodistal domain specification and interactions in developing *Drosophila* appendages. Development. 2001:**128**(12):2365–2372. https://doi.org/10.1242/dev.128.12.2365.
Donnadieu AL. Recherches pour servir a l'histoire des Tétranyques. Lyon, France: Académie de Lyon; 1875.
Dugès A. Recherches sur l'ordre des Acariens en général et la famille des Trombidiés en particular. Ann Sci Nat. 1834:**1**:5–46.
Eriksson BJ, Ungerer P, Stollewerk A. The function of Notch signalling in segment formation in the crustacean *Daphnia magna* (Branchiopoda). Dev Biol. 2013:**383**(2):321–330. https://doi.org/10.1016/j.ydbio.2013.09.021.
Evans GO. Principles of acarology. Wallingford: CAB International; 1992.
Fumouze A, Robin C. Mémoire anatomique et zoologique sur les Acariens des genres *Cheyletus, Glyciphagus* et *Tyroglyphus*. J Anat Physiol. 1867:**4**:561–601.
Gainett G, Crawford AR, Klementz BC, So C, Baker CM, Setton EVW, Sharma PP. Eggs to long-legs: embryonic staging of the harvestman *Phalangium opilio* (Opiliones), an emerging model arachnid. Front Zool. 2022:**19**(1):11. https://doi.org/10.1186/s12983-022-00454-z.
Gainett G, González VL, Ballesteros JA, Setton EVW, Baker CM, Gargiulo B, Santibáñez-López L, Coddington CE, Sharma JA, P P. The genome of a daddy-long-legs (opiliones) illuminates the evolution of arachnid appendages. Proc Biol Sci. 2021:**288**(1956):20211168. https://doi.org/10.1098/rspb.2021.1168.
Gainett G, Klementz BC, Blaszczyk P, Setton EVW, Murayama GP, Willemart R, Gavish-Regev E, Sharma PP. Vestigial organs alter fossil placements in an ancient group of terrestrial chelicerates. Curr Biol. 2024a:**34**(6):1258–1270. https://doi.org/10.1016/j.cub.2024.02.011.
Gainett G, Klementz BC, Setton EVW, Simian C, Iuri HA, Edgecombe GD, Peretti AV, Sharma PP. A plurality of morphological characters need not equate with phylogenetic accuracy: a rare genomic change refutes the placement of Solifugae and Pseudoscorpiones in Haplocnemata. Evol Dev. 2024b:**26**(4):e12467. https://doi.org/10.1111/ede.12467.
Gainett G, Sharma PP. Genomic resources and toolkits for developmental study of whip spiders (Amblypygi) provide insights into arachnid genome evolution and antenniform leg patterning. EvoDevo. 2020:**11**(1):18. https://doi.org/10.1186/s13227-020-00163-w.
Gout J-F, Hao Y, Johri P, Arnaiz O, Doak TG, Bhullar S, Couloux A, Guérin F, Malinsky S, Potekhin A, et al. Dynamics of gene loss following ancient whole-genome duplication in the cryptic *Paramecium* complex. Mol Biol Evol. 2023:**40**(5):msad107. https://doi.org/10.1093/molbev/msad107.
Grabherr MG, Haas BJ, Yassour M, Levin JZ, Thompson DA, Amit I, Adiconis X, Fan L, Raychowdhury R, Zeng Q, et al. Trinity: reconstructing a full-length transcriptome without a genome from RNA-Seq data. Nat Biotechnol. 2011:**29**(7):644–652. https://doi.org/10.1038/nbt.1883.
Haldane JB. The causes of evolution. Princeton (NJ): Princeton University Press; 1990.
Hall BK. Evolutionary developmental biology (Evo-Devo): past, present, and future. Evo Edu Outreach. 2012:**5**(2):184–193. https://doi.org/10.1007/s12052-012-0418-x.
Harvey M. The phylogeny and classification of the Pseudoscorpionida (Chelicerata: Arachnida). Invert Syst. 1992:**6**(6):1373. https://doi.org/10.1071/IT9921373.

Downloaded from https://academic.oup.com/mbe/article/41/9/msae188/7749772 by guest on 11 October 2024

Harvey MS. The Australian water mites: A guide to families and genera. Clayton (VIC): CSIRO Publishing; 1998.
He X, Zhang J. Rapid subfunctionalization accompanied by prolonged and substantial neofunctionalization in duplicate gene evolution. Genetics. 2005:**169**(2):1157–1164. https://doi.org/10.1534/genetics.104.037051.
Helfer H, Schlottke E. Pantopoda. Dr. HG Bronn's Klassen und Ordnung des Tierreichs, Band 5, Abt. IV, Buch 2. Leipzig: Akademische Verlagsgesellschaft m.b.H; 1935. p. 1–314.
Höch R, Schneider RF, Kickuth A, Meyer A, Woltering JM. Spiny and soft-rayed fin domains in acanthomorph fish are established through a BMP-*gremlin-shh* signaling network. Proc Natl Acad Sci U S A. 2021:**118**(29):29. https://doi.org/10.1073/pnas.2101783118.
Hoek PCC. Nouvelles études sur les Pycnogonides. Arch Zool Exp Gén. 1881:**9**:445–542.
Jager M, Murienne J, Clabaut C, Deutsch J, Guyader HL, Manuel M. Homology of arthropod anterior appendages revealed by Hox gene expression in a sea spider. Nature. 2006:**441**(7092):506–508. https://doi.org/10.1038/nature04591.
Janeschik M, Schacht MI, Platten F, Turetzek N. It takes two: discovery of spider *Pax2* duplicates indicates prominent role in chelicerate central nervous system, eye, as well as external sense organ precursor formation and diversification after neo- and subfunctionalization. Front Ecol Evol. 2022:**10**:810077. https://doi.org/10.3389/fevo.2022.810077.
Janssen R, Eriksson BJ, Budd GE, Akam M, Prpic N-M. Gene expression patterns in an onychophoran reveal that regionalization predates limb segmentation in pan-arthropods. Evol Dev. 2010:**12**(4):363–372. https://doi.org/10.1111/j.1525-142X.2010.00423.x.
Janssen R, Pechmann M, Turetzek N. A chelicerate Wnt gene expression atlas: novel insights into the complexity of arthropod Wnt-patterning. EvoDevo. 2021:**12**(1):12. https://doi.org/10.1186/s13227-021-00182-1.
Khadjeh S, Turetzek N, Pechmann M, Schwager EE, Wimmer EA, Damen WGM, Prpic N-M. Divergent role of the Hox gene *Antennapedia* in spiders is responsible for the convergent evolution of abdominal limb repression. Proc Natl Acad Sci U S A. 2012:**109**(13):4921–4926. https://doi.org/10.1073/pnas.1116421109.
King PE. Pycnogonids. London: Hutchinson; 1973.
Knowles DG, McLysaght A. Recent de novo origin of human protein-coding genes. Genome Res. 2009:**19**(10):1752–1759. https://doi.org/10.1101/gr.095026.109.
Krantz GW, Walter DE, Behan-Pelletier V, Cook DR, Harvey MS, Keirans JE, Lindquist EE, Norton RA, OConnor BM, Smith IM. A manual of acarology. In: Krantz GW, Walter DE, editors. 3rd ed. Lubbock (TX): Texas Tech University Press; 2009. p. 1–807.
Kuehn E, Clausen DS, Null RW, Metzger BM, Willis AD, Özpolat BD. Segment number threshold determines juvenile onset of germline cluster expansion in *Platynereis dumerilii*. J Exp Zool B. 2022:**338**(4):225–240. https://doi.org/10.1002/jez.b.23100.
Lynch M, Conery JS. The evolutionary fate and consequences of duplicate genes. Science. 2000:**290**(5494):1151–1155. https://doi.org/10.1126/science.290.5494.1151.
MacDonald ME, Hall BK. Altered timing of the extracellular-matrix-mediated epithelial-mesenchymal interaction that initiates mandibular skeletogenesis in three inbred strains of mice: development, heterochrony, and evolutionary change in morphology. J Exp Zool. 2001:**291**(3):258–273. https://doi.org/10.1002/jez.1102.
Mardon G, Solomon NM, Rubin GM. *Dachshund* encodes a nuclear protein required for normal eye and leg development in *Drosophila*. Development. 1994:**120**(12):3473–3486. https://doi.org/10.1242/dev.120.12.3473.
Mazo-Vargas A, Langmüller AM, Wilder A, van der Burg KRL, Lewis JJ, Messer PW, Zhang L, Martin A, Reed RD. Deep *cis*-regulatory homology of the butterfly wing pattern ground plan. Science. 2022:**378**(6617):304–308. https://doi.org/10.1126/science.abi9407.
Meinert F. Pycnogonida. In: The Danish Ingolf-Expedition. 3rd ed. Copenhagen, Denmark: H. Hagerup; 1899. p. 1–71.
Michael AD. British Oribatidae. London: Ray Society; 1884.
Michalski H, Harms D, Runge J, Wirkner CS. Evolutionary morphology of coxal musculature in Pseudoscorpiones (Arachnida). Arthropod Struct Dev. 2022:**69**:101165. https://doi.org/10.1016/j.asd.2022.101165.
Millot J. Ordre des solifuges. In: Grassé P-P, editors. Traité de zoologie. Vol. 6. Paris: Masson; 1949. p. 482–519.
Mito T, Ronco M, Uda T, Nakamura T, Ohuchi H, Noji S. Divergent and conserved roles of *extradenticle* in body segmentation and appendage formation, respectively, in the cricket *Gryllus bimaculatus*. Dev Biol. 2008:**313**(1):67–79. https://doi.org/10.1016/j.ydbio.2007.09.060.
Moczek AP, Rose DJ. Differential recruitment of limb patterning genes during development and diversification of beetle horns. Proc Natl Acad Sci U S A. 2009:**106**(22):8992–8997. https://doi.org/10.1073/pnas.0809668106.
Nguyen L-T, Schmidt HA, von Haeseler A, Minh BQ. IQ-TREE: a fast and effective stochastic algorithm for estimating maximum-likelihood phylogenies. Mol Biol Evol. 2015:**32**(1):268–274. https://doi.org/10.1093/molbev/msu300.
Nicolet MH. Histoire naturelle des acariens qui se trouvent aux environs de Paris. Paris, France: Mallet; 1855. p. 11–36.
Nolan ED, Santibáñez-López CE, Sharma PP. Developmental gene expression as a phylogenetic data class: support for the monophyly of Arachnopulmonata. Dev Genes Evol. 2020:**230**(2):137–153. https://doi.org/10.1007/s00427-019-00644-6.
Nong W, Qu Z, Li Y, Barton-Owen T, Wong AYP, Yip HY, Lee HT, Narayana S, Baril T, Swale T, et al. Horseshoe crab genomes reveal the evolution of genes and microRNAs after three rounds of whole genome duplication. Commun Biol. 2021:**4**(1):83–11. https://doi.org/10.1038/s42003-020-01637-2.
Nuss AB, Lomas JS, Reyes JB, Garcia-Cruz O, Lei W, Sharma A, Pham MN, Beniwal S, Swain ML, McVicar M, et al. The highly improved genome of *Ixodes scapularis* with X and Y pseudochromosomes. Life Sci Alliance. 2023:**6**(12):e202302109. https://doi.org/10.26508/lsa.202302109.
Ohno S. Evolution by gene duplication. New York (NY): Springer; 1970.
Ontano AZ, Gainett G, Aharon S, Ballesteros JA, Benavides LR, Corbett KF, Gavish-Regev E, Harvey MS, Monsma S, Santibáñez-López CE, et al. Taxonomic sampling and rare genomic changes overcome long-branch attraction in the phylogenetic placement of pseudoscorpions. Mol Biol Evol. 2021:**38**(6):2446–2467. https://doi.org/10.1093/molbev/msab038.
Pechmann M, Prpic N-M. Appendage patterning in the South American bird spider *Acanthoscurria geniculata* (Araneae: Mygalomorphae). Dev Genes Evol. 2009:**219**(4):189–198. https://doi.org/10.1007/s00427-009-0279-7.
Pittard K, Mitchell RW. Comparative morphology of the life stages of Cryptocellus pelaezi (Arachnida, Ricinulei). Graduate Studies, Texas Tech University. 1972:**1**:1–78.
Prpic N-M, Damen WGM. Notch-mediated segmentation of the appendages is a molecular phylotypic trait of the arthropods. Dev Biol. 2009:**326**(1):262–271. https://doi.org/10.1016/j.ydbio.2008.10.049.
Prpic N-M, Janssen R, Wigand B, Klingler M, Damen WGM. Gene expression in spider appendages reveals reversal of exd/hth spatial specificity, altered leg gap gene dynamics, and suggests divergent morphogen signaling. Dev Biol. 2003:**264**(1):119–140. https://doi.org/10.1016/j.ydbio.2003.08.002.
Prpic N-M, Tautz D. The expression of the proximodistal axis patterning genes *Distal-less* and *dachshund* in the appendages of *Glomeris marginata* (Myriapoda: Diplopoda) suggests a special role of these genes in patterning the head appendages. Dev Biol. 2003:**260**(1):97–112. https://doi.org/10.1016/S0012-1606(03)00217-3.
Pueyo JI, Lanfear R, Couso JP. Ancestral Notch-mediated segmentation revealed in the cockroach *Periplaneta americana*. Proc Natl Acad Sci U S A. 2008:**105**(43):16614–16619. https://doi.org/10.1073/pnas.0804093105.
Punzo F. The biology of Camel-Spiders (Arachnida, Solifugae). Norwell (MA): Kluwer Academic Publishers; 1998.

Downloaded from https://academic.oup.com/mbe/article/41/9/msae188/7749772 by guest on 11 October 2024

Raff RA. Direct-developing sea urchins and the evolutionary reorganization of early development. BioEssays. 1992:**14**(4):211–218. https://doi.org/10.1002/bies.950140403.
Rauskolb C. The establishment of segmentation in the *Drosophila* leg. Development. 2001:**128**(22):4511–4521. https://doi.org/10.1242/dev.128.22.4511.
Rauskolb C, Irvine KD. Notch-mediated segmentation and growth control of the *Drosophila* leg. Dev Biol. 1999:**210**(2):339–350. https://doi.org/10.1006/dbio.1999.9273.
Rauskolb C, Smith KM, Peifer M, Wieschaus E. *Extradenticle* determines segmental identities throughout *Drosophila* development. Development. 1995:**121**(11):3663–3673. https://doi.org/10.1242/dev.121.11.3663.
Regier JC, Shultz JW, Zwick A, Hussey A, Ball B, Wetzer R, Martin JW, Cunningham CW. Arthropod relationships revealed by phylogenomic analysis of nuclear protein-coding sequences. Nature. 2010:**463**(7284):1079–1083. https://doi.org/10.1038/nature08742.
Reyes J, Ayala-Chavez C, Sharma A, Pham M, Nuss AB, Gulia-Nuss M. Blood digestion by trypsin-like serine proteases in the replete Lyme disease vector tick, *Ixodes scapularis*. Insects. 2020:**11**(3):201. https://doi.org/10.3390/insects11030201.
Sabroux R, Edgecombe GD, Pisani D, Garwood RJ. New insights into the sea spider fauna (Arthropoda, Pycnogonida) of La Voulte-sur-Rhône, France (Jurassic, Callovian). Pap Palaeontol. 2023:**9**(4):e1515. https://doi.org/10.1002/spp2.1515.
Sánchez EC, López-González PJ. Postembryonic development of *Nymphon unguiculatum* Hodgson 1915 (Pycnogonida, Nymphonidae) from the South Shetland Islands (Antarctica). Polar Biol. 2010:**33**(9):1205–1214. https://doi.org/10.1007/s00300-010-0810-3.
Sars GO. Pycnogonidea. In: Norwegian North-Atlantic expedition, 1876–1878. Oslo, Norway: Christiana, Grøndahl & Søns Bogtrykkeri; 1891. p. 1–163.
Savory T. Arachnida. London: Academic Press Inc.; 1964.
Schram FR, Hedgpeth JW. Locomotory mechanisms in Antarctic pycnogonids. Zool J Linn Soc. 1978:**63**(1-2):145–170. https://doi.org/10.1111/j.1096-3642.1978.tb02095.x.
Selden PA. Functional morphology of the prosoma of *Baltoeurypterus tetragonophthalmus* (Fischer) (Chelicerata: Eurypterida). Trans Roy Soc Edinb: Earth Sci. 1981:**72**(1):9–48. https://doi.org/10.1017/S0263593300003217.
Setton EVW, Sharma PP. Cooption of an appendage-patterning gene cassette in the head segmentation of arachnids. Proc Natl Acad Sci U S A. 2018:**115**(15):E3491–E3500. https://doi.org/10.1073/pnas.1720193115.
Sewell W, Williams T, Cooley J, Terry M, Ho R, Nagy L. Evidence for a novel role for *dachshund* in patterning the proximal arthropod leg. Dev Genes Evol. 2008:**218**(6):293–305. https://doi.org/10.1007/s00427-008-0220-5.
Sharma PP. The impact of whole genome duplication on the evolution of the arachnids. Integr Comp Biol. 2023:**63**(3):825–842. https://doi.org/10.1093/icb/icad050.
Sharma PP, Kaluziak ST, Pérez-Porro AR, González VL, Hormiga G, Wheeler WC, Giribet G. Phylogenomic interrogation of Arachnida reveals systemic conflicts in phylogenetic signal. Mol Biol Evol. 2014:**31**(11):2963–2984. https://doi.org/10.1093/molbev/msu235.
Sharma A, Pham MN, Reyes JB, Yim CR, Heu WC, Kim CC, Chaverra-Rodriguez D, Rasgon D, Harrell JL, A R, et al. Cas9-mediated gene editing in the black-legged tick, *Ixodes scapularis*, by embryo injection and ReMOT control. iScience. 2022:**25**(3):103781. https://doi.org/10.1016/j.isci.2022.103781.
Sharma PP, Schwager EE, Extavour CG, Giribet G. Evolution of the chelicera: a *dachshund* domain is retained in the deutocerebral appendage of Opiliones (Arthropoda, Chelicerata). Evol Dev. 2012a:**14**(6):522–533. https://doi.org/10.1111/ede.12005.
Sharma PP, Schwager EE, Extavour CG, Giribet G. Hox gene expression in the harvestman *Phalangium opilio* reveals divergent patterning of the chelicerate opisthosoma. Evol Dev. 2012b:**14**(5):450–463. https://doi.org/10.1111/j.1525-142X.2012.00565.x.
Sharma PP, Schwager EE, Giribet G, Jockusch EL, Extavour CG. *Distal-less* and *dachshund* pattern both plesiomorphic and apomorphic structures in chelicerates: RNA interference in the harvestman *Phalangium opilio* (Opiliones). Evol Dev. 2013:**15**(4):228–242. https://doi.org/10.1111/ede.12029.
Shear WA, Selden PA, Rolfe WDI, Bonamo PM, Grierson JD. New terrestrial arachnids from the Devonian of Gilboa, New York (Arachnida, Trigonotarbida). Am Mus Novit. 1987:**2901**:1–74.
Shultz JW. Morphology of locomotor appendages in Arachnida: evolutionary trends and phylogenetic implications. Zool J Linn Soc. 1989:**97**(1):1–55. https://doi.org/10.1111/j.1096-3642.1989.tb00552.x.
Sievers F, Higgins DG. Clustal Omega for making accurate alignments of many protein sequences. Protein Sci. 2018:**27**(1):135–145. https://doi.org/10.1002/pro.3290.
Smith KK. Beyond heterochrony: the evolution of development. Heredity (Edinb). 2003:**90**(1):8–8. https://doi.org/10.1038/sj.hdy.6800197.
Smith FW, Jockusch EL. Hox genes require *homothorax* and *extradenticle* for body wall identity specification but not for appendage identity specification during metamorphosis of *Tribolium castaneum*. Dev Biol. 2014:**395**(1):182–197. https://doi.org/10.1016/j.ydbio.2014.08.017.
Snodgrass RE. Evolution of arthropod mechanisms. Washington DC, USA: Smithsonian Miscellaneous Collections; 1958.
Stollewerk A. Recruitment of cell groups through Delta/Notch signaling during spider neurogenesis. Development. 2002:**129**(23):5339–5348. https://doi.org/10.1242/dev.00109.
Stollewerk A, Schoppmeier M, Damen WGM. Involvement of *Notch* and *Delta* genes in spider segmentation. Nature. 2003:**423**(6942):863–865. https://doi.org/10.1038/nature01682.
Sugime Y, Oguchi K, Gotoh H, Hayashi Y, Matsunami M, Shigenobu S, Koshikawa S, Miura T. Termite soldier mandibles are elongated by *dachshund* under hormonal and Hox gene controls. Development. 2019:**146**(5):dev171942. https://doi.org/10.1242/dev.171942.
Sutton MD, Briggs DEG, Siveter David J, Siveter Derek J, Orr PJ. The arthropod *Offacolus kingi* (Chelicerata) from the Silurian of Herefordshire, England: computer based morphological reconstructions and phylogenetic affinities. Proc Biol Sci. 2002:**269**(1497):1195–1203. https://doi.org/10.1098/rspb.2002.1986.
Tendolkar A, Mazo-Vargas A, Livraghi L, Hanly JJ, Horne KCV, Gilbert LE, Martin A. *Cis*-regulatory modes of *Ultrabithorax* inactivation in butterfly forewings. eLife. 2024:**12**:RP90846. https://doi.org/10.7554/eLife.90846.
Tills O, Rundle SD, Salinger M, Haun T, Pfenninger M, Spicer JI. A genetic basis for intraspecific differences in developmental timing? Evol Dev. 2011:**13**(6):542–548. https://doi.org/10.1111/j.1525-142X.2011.00510.x.
Turetzek N, Khadjeh S, Schomburg C, Prpic N-M. Rapid diversification of homothorax expression patterns after gene duplication in spiders. BMC Evol Biol. 2017:**17**(1):168. https://doi.org/10.1186/s12862-017-1013-0.
Turetzek N, Pechmann M, Schomburg C, Schneider J, Prpic N-M. Neofunctionalization of a duplicate *dachshund* gene underlies the evolution of a novel leg segment in arachnids. Mol Biol Evol. 2016:**33**(1):109–121. https://doi.org/10.1093/molbev/msv200.
van der Hammen L. La segmentation des appendices chez les acariens. Acarologia. 1970:**12**(1):11–15.
van der Hammen L. A new classification of Chelicerata. Zool Meded. 1977:**51**:307–319.
van der Hammen L. Comparative studies in Chelicerata II. Epimerata (Palpigradi and Actinotrichida). Zool Verh. 1982:**196**:1–70.
van der Hammen L. A structural approach in the study of evolution and classification. Zool Meded. 1985:**59**:392–409.
van der Hammen L. Acarological and arachnological notes. Zool Meded. 1986:**60**:217–230.
Vilpoux K, Waloszek D. Larval development and morphogenesis of the sea spider *Pycnogonum litorale* (Ström, 1762) and the tagmosis of the body of Pantopoda. Arthropod Struct Dev. 2003:**32**(4):349–383. https://doi.org/10.1016/j.asd.2003.09.004.

Downloaded from https://academic.oup.com/mbe/article/41/9/msae188/7749772 by guest on 11 October 2024